Article

The Reactivity Patterns of Low-Coordinate Iron#Hydride Complexes

Ying Yu, Azwana R. Sadique, Jeremy M. Smith, Thomas R. Dugan, Ryan E. Cowley, William W. Brennessel, Christine J. Flaschenriem, Eckhard Bill, Thomas R. Cundari, and Patrick L. Holland

J. Am. Chem. Soc., **2008**, 130 (20), 6624-6638 • DOI: 10.1021/ja710669w • Publication Date (Web): 30 April 2008

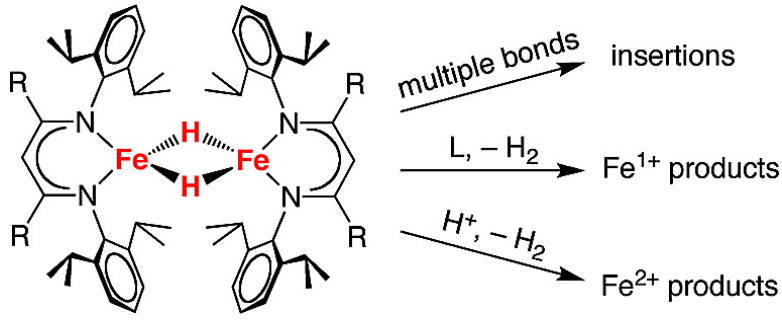

More About This Article

Additional resources and features associated with this article are available within the HTML version:

- Supporting Information
- Links to the 2 articles that cite this article, as of the time of this article download
- Access to high resolution figures
- Links to articles and content related to this article
- Copyright permission to reproduce figures and/or text from this article

View the Full Text HTML

J|A|C|S
ARTICLES

Published on Web 04/30/2008

The Reactivity Patterns of Low-Coordinate Iron−Hydride Complexes

Ying Yu, Azwana R. Sadique, Jeremy M. Smith, Thomas R. Dugan, Ryan E. Cowley, William W. Brennessel, Christine J. Flaschenriem, Eckhard Bill, Thomas R. Cundari,* and Patrick L. Holland*

Department of Chemistry, University of Rochester, Rochester, New York, 14627, Max-Planck-Institut für Bioanorganische Chemie, D-45470 Mülheim an der Ruhr, Germany, Department of Chemistry and Center for Advanced Scientific Computing and Modeling (CASCaM), University of North Texas, Denton, Texas, 76203

Received November 28, 2007; E-mail: holland@chem.rochester.edu; tomc@unt.edu

Abstract: We report a survey of the reactivity of the first isolable iron-hydride complexes with a coordination number less than 5. The high-spin iron(II) complexes [(β-diketiminate)Fe(μ-H)]$_2$ react rapidly with representative cyanide, isocyanide, alkyne, N_2, alkene, diazene, azide, CO_2, carbodiimide, and Brønsted acid containing substrates. The reaction outcomes fall into three categories: (1) addition of Fe−H across a multiple bond of the substrate, (2) reductive elimination of H_2 to form iron(I) products, and (3) protonation of the hydride to form iron(II) products. The products include imide, isocyanide, vinyl, alkyl, azide, triazenido, benzo[*c*]cinnoline, amidinate, formate, and hydroxo complexes. These results expand the range of known bond transformations at iron complexes. Additionally, they give insight into the elementary transformations that may be possible at the iron−molybdenum cofactor of nitrogenases, which may have hydride ligands on high-spin, low-coordinate metal atoms.

Introduction

Organometallic chemists have long appreciated the many reactions of transition-metal hydride complexes, especially reductions.[1] Recently, hydride chemistry has become established in bioinorganic systems.[2] Nitrogenases are prodigious reductants that cleave double and triple bonds in N_2, CO_2, N_2O, N_3^-, and CN^- at iron−sulfur clusters (FeMoco in the molybdenum−iron nitrogenases, FeVco in the vanadium−iron nitrogenases, and FeFeco in the iron-only nitrogenases).[3] Because these substrates are reduced by multiples of two electrons accompanied by the addition of protons, chemists have often speculated about the potential role of hydrides.[4]

Recently, the first direct evidence for hydride intermediates in nitrogenase emerged from electron−nuclear double resonance (ENDOR) studies of nitrogenase mutants freeze-trapped during substrate turnover. For example, a Val70Ile mutant of *A. vinelandii* molybdenum−iron nitrogenase freeze-trapped during proton reduction shows two hydrogen nuclei with very strong coupling to the $S = {}^1/_2$ iron−sulfur cluster, strongly suggesting the presence of Fe−H bonds.[5] This frozen species loses two molecules of H_2 upon annealing to −20 °C, raising the possibility that these two hydride ligands can combine with nearby protons to release H_2.[6] This species is thought to be in the redox state that reacts directly with N_2 in the wild-type MoFe nitrogenase,[7] underscoring the importance of hydride-containing intermediates in enabling the nitrogen reduction activity characteristic of this enzyme.

From the perspective of the coordination chemist, there are a number of ways that potential FeMoco-bound hydrides differ from the majority of known synthetic transition-metal hydride complexes. First, FeMoco hydride adducts could achieve a number of different oxidation levels. One-electron redox changes undoubtedly occur in the FeMoco because electrons are supplied to the FeMoco one at a time by the Fe protein, which dissociates and reassociates before each one-electron reduction of the FeMoco.[3] However, most synthetic hydride complexes have diamagnetic metal centers, and little one-electron chemistry has

(1) (a) *Recent Advances in Hydride Chemistry*; Peruzzini, M., Poli, R., Eds.; Elsevier: New York, 2001. (b) McGrady, G. S.; Guilera, G. *Chem. Soc. Rev.* **2003**, *32*, 383–392.
(2) (a) Especially rapid progress has occurred in the area of hydrogenase structure and reactivity : Maroney, M. J. *J. Biol. Inorg. Chem.* **2001**, *6*, 452. (b) Nicolet, Y.; Cavazza, C.; Fontecilla-Camps, J. C. *J. Inorg. Biochem.* **2002**, *91*, 1–8. (c) Armstrong, F. A. *Curr. Opin. Chem. Biol.* **2004**, *8*, 133–140. (d) Liu, X.; Ibrahim, S. K.; Tard, C.; Pickett, C. J. *Coord. Chem. Rev.* **2005**, *249*, 1641–1652.
(3) (a) Howard, J. B.; Rees, D. C. *Chem. Rev.* **1996**, *96*, 2965–2982. (b) Burgess, B. K.; Lowe, D. J. *Chem. Rev.* **1996**, *96*, 2983–3011. (c) Eady, R. R. *Chem. Rev.* **1996**, *96*, 3013–3030. (d) Holland, P. L. Nitrogen Fixation. In *Comprehensive Coordination Chemistry II*; McCleverty, J., Meyer, T. J., Eds.; Elsevier: Oxford, U.K., 2004; Vol. 8, pp 569−599.
(4) (a) Thorneley, R. N. F.; Eady, R. R.; Lowe, D. J. *Nature* **1978**, *272*, 557–558. (b) Leigh, G. J.; McMahon, C. N. *J. Organomet. Chem.* **1995**, *500*, 219–225. (c) Henderson, R. A. In *Recent Advances in Hydride Chemistry;* Peruzzini, M., Poli, R., Eds.; Elsevier: New York, 2001; pp 463−505. (d) Dance, I. *Biochemistry* **2006**, *45*, 6328–6340.
(5) Igarashi, R. Y.; Laryukhin, M.; Dos Santos, P. C.; Lee, H.-I.; Dean, D. R.; Seefeldt, L. C.; Hoffman, B. M. *J. Am. Chem. Soc.* **2005**, *127*, 6231–6241.
(6) Lukoyanov, D.; Barney, B. M.; Dean, D. R.; Seefeldt, L. C.; Hoffman, B. M. *Proc. Natl. Acad. Sci. U.S.A.* **2007**, *104*, 1451–1455.
(7) Thorneley, R. N. F.; Lowe, D. J. *Met. Ions Biol.* **1985**, *7*, 221–284.
(8) Einsle, O.; Tezcan, F. A.; Andrade, S. L. A.; Schmid, B.; Yoshida, M.; Howard, J. B.; Rees, D. C. *Science* **2002**, *297*, 1696–1700.

 10.1021/ja710669w CCC: $40.75

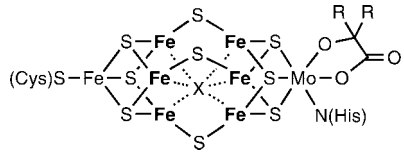

Figure 1. The iron−molybdenum cofactor ("FeMoco") of iron−molybdenum nitrogenase in the isolated M^N form.[8] This form is reduced (with incorporation of hydrides in an undisclosed location) to give the intermediate that reacts with N_2 and other nitrogenase substrates. X is C^{4-}, N^{3-}, or O^{2-}.

been reported.[9,10] Second, the iron ions in the FeMoco are expected to be high-spin, based on ligand field considerations (weak-field sulfide donor set, coordination number less than five) and the results of computational studies.[11] Synthetic hydride complexes, on the other hand, typically have strong-field organometallic or phosphine coligands, which enforce a low-spin electronic configuration.[12,13] These fundamental differences motivate synthetic research aimed at the creation of iron−hydride complexes with weak-field ligands and low coordination number, to determine their characteristic reactivity patterns and reaction mechanisms, which can in turn be correlated with nitrogenase reactions.

Often the design of functional models of an enzyme is driven by an attempt to achieve structural similarity to the enzyme's active site.[14] In the case of nitrogenase, an accurate structural mimic of the FeMoco hydride species is elusive for several reasons. First, the FeMoco of iron−molybdenum nitrogenase (Figure 1) has eight transition metals in a cluster type (M_8S_9C or M_8S_9N or M_8S_9O) that is unknown in synthetic chemistry.[15,16] Second, the *crystallographically characterized* form of the FeMoco (M^N) does not have hydrides, as shown by ENDOR: hydrides are only incorporated concurrent with catalytic turnover.[5] In any case, X-ray crystal structures of proteins do not have sufficient resolution to distinguish hydrogen atoms. Third, the N_2-binding form of the FeMoco is reduced by three to four electrons from M^N, and the FeMoco may undergo structural

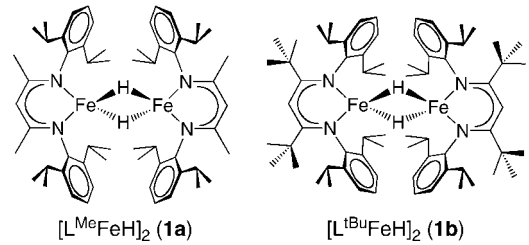

Figure 2. Bulky β-diketiminate iron complexes used in this work. The ligands are abbreviated L^R, where R is the group on the diketiminate backbone. Both complexes have roughly tetrahedral geometry at each iron atom.[20,21]

rearrangements upon reduction.[7,17] Peters and Holland have independently proposed that dissociation of X is important in enabling substrate binding to iron, based on the binding of N_2 to synthetic iron complexes.[18] Computational studies come to a variety of conclusions regarding the structural flexibility of the FeMoco during catalysis.[11] In short, there are many questions about the structure of the iron−hydride nitrogenase intermediates, and the available data are not sufficient to provide guesses about their structure(s).

For these reasons, we have created one- and two-iron compounds that focus on two key features of the nitrogenase-hydride intermediates: the weak-field ligands and the coordination number less than five.[18a] Extremely bulky bidentate β-diketiminate ligands (Figure 2) have π-donating nitrogen atoms that lead to a weak ligand field.[19] The bulky diisopropylphenyl groups maintain a low coordination number that mimics the ligand-poor environment of the iron atoms in the FeMoco. Using these ligands, we have isolated *the only examples of iron-hydride complexes with a coordination number less than five* (Figure 2).[20,21]

Our studies on low-coordinate iron are complemented by those of Peters and co-workers, who use tridentate, strong-field tris(phosphino)borate (BP_3) supporting ligands that contain "soft" phosphine donors, and more often give low-spin electronic configurations.[22] In the BP_3 systems, it has not yet been possible to isolate a low-coordinate iron hydride, but the presence of a terminal hydride in four-coordinate complexes is strongly

(9) Poli, R. Paramagnetic Mono- and Polyhydrides of the Transition Metals. In *Recent Advances in Hydride Chemistry;* Peruzzini, M., Poli, R., Eds.; Elsevier: New York, 2001, pp 139−188.
(10) (a) Two examples of paramagnetic iron−hydride complexes: Gargano, M.; Giannoccaro, P.; Rossi, M.; Vasapollo, G.; Sacco, A. *J. Chem. Soc., Dalton Trans.* **1975**, 9–12. (b) Rakowski, M. C.; Busch, D. H. *J. Am. Chem. Soc.* **1975**, *97*, 2570–2571.
(11) (a) Dance, I. *Chem. Commun.* **2003**, 324–325. (b) Hinnemann, B.; Nørskov, J. K. *J. Am. Chem. Soc.* **2003**, *125*, 1466–1467. (c) Lovell, T.; Liu, T.; Case, D. A.; Noodleman, L. *J. Am. Chem. Soc.* **2003**, *125*, 8377–8383. (d) Schimpl, J.; Petrilli, H. M.; Blöchl, P. E. *J. Am. Chem. Soc.* **2003**, *125*, 15772–15778. (e) Huniar, U.; Ahlrichs, R.; Coucouvanis, D. *J. Am. Chem. Soc.* **2004**, *126*, 2588–2601. (f) Hinnemann, B.; Nørskov, J. K. *J. Am. Chem. Soc.* **2004**, *126*, 3920–3927. (g) Kästner, J.; Hemmen, S.; Blöchl, P. E. *J. Chem. Phys.* **2005**, *123*, 074306. (h) Dance, I. *J. Am. Chem. Soc.* **2007**, *129*, 1076–1088. (i) Kästner, J.; Blöchl, P. E. *J. Am. Chem. Soc.* **2007**, *129*, 2998–3006. (j) McKee, M. L. *J. Comput. Chem.* **2007**, *28*, 1796–1808.
(12) (a) $[Cp^*Fe(dppe)H]^+$: Hamon, P.; Toupet, L.; Hamon, J. R.; Lapinte, C. *Organometallics* **1992**, *11*, 1429–1431. (b) Hamon, P.; Hamon, J. R.; Lapinte, C. *J. Chem. Soc., Chem. Commun.* **1992**, 1602–1603.
(13) The hydride ligand itself is a fairly strong-field ligand: Linn, D. E., Jr.; Gibbins, S. G. *Inorg. Chem.* **1997**, *36*, 3461–3465.
(14) Ibers, J. A.; Holm, R. H. *Science* **1980**, *209*, 223–235.
(15) (a) Review: Lee, S. C.; Holm, R. H. *Proc. Natl. Acad. Sci. U.S.A.* **2003**, *100*, 3595–3600. (b) Recent progress: Ohki, Y.; Ikagawa, Y.; Tatsumi, K. *J. Am. Chem. Soc.* **2007**, *129*, 10457–10465.
(16) Nitrogenase enzymes without Mo probably have a similarly-shaped clusters, based on X-ray absorption results : Krahn, E.; Weiss, B. J. R.; Kröckel, M.; Groppe, J.; Henkel, G.; Cramer, S. P.; Trautwein, A. X.; Schneider, K.; Müller, A. *J. Biol. Inorg. Chem.* **2002**, *7*, 37–45.
(17) Extracted FeMoco is structurally intact but inactive. See ref 3b.
(18) (a) Holland, P. L. *Can. J. Chem.* **2005**, *83*, 296–301. (b) Peters, J. C.; Mehn, M. P. Bio-organometallic approaches to nitrogen fixation chemistry. In *Activation of Small Molecules* Tolman, W. B., Ed.; Wiley: Weinheim, Germany, 2006; pp 81−119.
(19) The electronic structure of trigonal-planar diketiminate-iron complexes: Andres, H.; Bominaar, E.; Smith, J. M.; Eckert, N. A.; Holland, P. L.; Münck, E, *J. Am. Chem. Soc.* **2002**, *124*, 3012–3025. (b) Holland, P. L.; Cundari, T. R.; Perez, L. L.; Eckert, N. A.; Lachicotte, R. J. *J. Am. Chem. Soc.* **2002**, *124*, 14416–14424. (c) Stoian, S. A.; Yu, Y.; Smith, J. M.; Holland, P. L.; Bominaar, E. L.; Münck, E. *Inorg. Chem.* **2005**, *44*, 4915–4922. (d) Stoian, S. A.; Vela, J.; Smith, J. M.; Sadique, A. R.; Holland, P. L.; Münck, E.; Bominaar, E. L. *J. Am. Chem. Soc.* **2006**, *128*, 10181–10192.
(20) Smith, J. M.; Lachicotte, R. J.; Holland, P. L. *J. Am. Chem. Soc.* **2003**, *125*, 15752–15753.
(21) Vela, J.; Smith, J. M.; Yu, Y.; Ketterer, N. A.; Flaschenriem, C. J.; Lachicotte, R. J.; Holland, P. L. *J. Am. Chem. Soc.* **2005**, *127*, 7857–7870.
(22) (a) Betley, T. A.; Peters, J. C. *J. Am. Chem. Soc.* **2003**, *125*, 10782–10783. (b) Betley, T. A.; Peters, J. C. *Inorg. Chem.* **2003**, *42*, 5074–5084. (c) Jenkins, D. M.; Peters, J. C. *J. Am. Chem. Soc.* **2003**, *125*, 11162–11163. (d) Betley, T. A.; Peters, J. C. *J. Am. Chem. Soc.* **2004**, *126*, 6252–6254. (e) Thomas, C. M.; Peters, J. C. *Inorg. Chem.* **2004**, *43*, 8–10. (f) Jenkins, D. M.; Peters, J. C. *J. Am. Chem. Soc.* **2005**, *127*, 7148–7165. (g) Hendrich, M. P.; Gunderson, W.; Behan, R. K.; Green, M. T.; Mehn, M. P.; Betley, T. A.; Lu, C. C.; Peters, J. C. *Proc. Natl. Acad. Sci. U.S.A.* **2006**, *103*, 17107–17112.

implied by the isolation of products that result from activation of solvent or the supporting ligand.[23] Bridging hydrides have recently been observed in a few electronically unsaturated dinuclear complexes,[24,25] and borohydrides have been studied on iron−sulfur clusters.[26]

Recent contributions from our group have described the reaction of $[L^{tBu}FeH]_2$ with azobenzene to cleave the N═N bond,[20,27] and the reaction of $[L^{Me}FeH]_2$ with boranes to cleave B−C bonds.[28] This manuscript reports a wider variety of reactions with unsaturated small molecules that are nitrogenase substrates or organic-soluble mimics of these substrates. By examining the reactions with representative compounds, one may begin to understand some of the unusual reaction patterns available to hydride complexes with a high-spin electronic configuration. In addition, a number of the products have novel structural and/or electronic features that are interesting from a fundamental perspective.

Results

Iron-Hydride Starting Materials. The synthesis and characterization of $[L^{Me}FeH]_2$ (**1a**) and $[L^{tBu}FeH]_2$ (**1b**) have been presented previously.[20,21,27,28] They are each synthesized from iron(II) chloride complexes ($[L^{Me}FeCl]_2$ or $L^{tBu}FeCl$) by reaction with potassium triethylborohydride for 0.5 h in toluene, followed by the prompt removal of solvent and BEt_3, then extraction with pentane and crystallization to give brown powders or crystals. Crude reaction mixtures are contaminated with the chloride starting material and the dihydridoborate complex $L^RFe(\mu\text{-}H)_2BEt_2$.[28] Multiple crystallizations are typically necessary to remove these impurities, and ^{1}H NMR spectroscopy is used to judge purity of the hydride complexes. The good yields of many of the products derived therefrom support the purity of **1a** and **1b**.

The ^{1}H NMR spectrum of **1a** consists of seven resonances; the number of signals and their integrations are characteristic of the diketiminate ligand in a local C_{2v} symmetry environment. It has no unusual temperature- or concentration-dependent changes in its ^{1}H NMR or UV−vis spectra, suggesting that the dimeric structure in the solid state is always maintained. To learn more about the electronic structure of **1a**, we examined a solid sample using Mössbauer spectroscopy. The zero-field Mössbauer spectrum at 80 K (Supporting Information, Figure S-6) exhibits a superposition of two quadrupole doublets with 72% and 28% relative intensities. The major component has $\delta = 0.70(2)$ mm/s and $\Delta E_Q = 0.86(2)$ mm/s, whereas the minor component shows $\delta = 0.49(2)$ mm/s and $\Delta E_Q = 2.06(2)$ mm/s. The values for the minor component are relatively similar to those of a high-spin Fe(I) diketiminate complex ($\Delta E_Q = 2.02$ mm/s, $\delta = 0.41$ mm/s at 180 K).[19c] Therefore, we assign the component to contamination from an unidentified Fe(I) impurity. In contrast, the Mössbauer parameters of the major component, particularly the isomer shift, are in the range of high-spin iron(II) diketiminate complexes ($\delta = 0.62-0.86$ mm/s), and so it is assigned to **1a**.[19,29] Magnetic Mössbauer spectra measured at 4.2 K with applied fields up to 7 T show that the major component is diamagnetic, suggesting antiferromagnetic coupling between the two iron(II) ions. In sum, the spectroscopic data support the formulation of **1a** as an exchange-coupled pair of high-spin iron(II) ions with a ground state of $S = 0$.

The ^{1}H NMR spectrum of **1b** has at least 17 overlapping peaks, because of extreme steric crowding in the dimer that presumably renders some ligand bond rotations slow on the NMR time scale.[27] Upon heating a solution of **1b** in C_6D_6, there is growth of a simple seven-line ^{1}H NMR spectrum with chemical shifts much like trigonal-planar alkyl complexes $L^{tBu}FeR$.[20] This behavior is ascribable to equilibration between dimeric $[L^{tBu}FeH]_2$ and monomeric $L^{tBu}FeH$ that is slow on the NMR time scale (ms) but rapid on the time scale of the equilibration (min). Therefore, in the discussion below it should be understood that **1b** does not refer specifically to the monomer or dimer, but the equilibrating mixture of the two.[30]

Reactions with C≡N Triple Bonds, and with N_2 and CO. Carbon monoxide (CO) is an inhibitor of N_2 reduction by nitrogenase.[3] Methyl isocyanide (CH_3NC) and cyanide (CN^-) are also inhibitors but are substrates as well: CN^- is reduced to CH_3NH_2, NH_3, and CH_4, while CH_3NC is reduced to CH_3NH_2, $(CH_3)_2NH$, and CH_4.[31] Therefore, it is of interest to examine the reactivity of small molecules containing CO and CN triple bonds with synthetic hydride complexes that mimic potential activated forms of the FeMoco. We use alkyl cyanides as surrogates for CN^- and *tert*-butyl isocyanide in place of CH_3NC.

The addition of CO or isocyanide to **1a** results in the rapid release of H_2. Adding an excess of CO to **1a** gives $L^{Me}Fe(CO)_3$ through formal reduction of the iron. Because $L^{Me}Fe(CO)_3$ has been characterized previously, the reader is referred to the earlier paper for its properties.[47]

Addition of a large excess of *tert*-butyl isocyanide gives an intractable mixture, but treatment of a solution of **1a** in pentane or toluene with 4 equiv (per dimer) of *tert*-butyl isocyanide results in the formation of a mononuclear iron(I) complex, $L^{Me}Fe(CN^tBu)_2$ (**2a**). Integration of the ^{1}H NMR spectrum against an internal standard ($L^{tBu}FeCl$ in a capillary) indicated 62% conversion to **2a**, among other unidentified products. The production of H_2 was quantified by GC to be ca. 0.2 equiv per mole of **1a**. The low yield of dihydrogen may be due to hydrogen incorporation into some of the unidentified products. Because of the low conversion, samples of **2a** for further spectroscopic study were generated through an alternative method, by adding 4 equiv of ^{t}BuNC to $L^{Me}FeNNFeL^{Me}$. The

(23) (a) Brown, S. D.; Peters, J. C. *J. Am. Chem. Soc.* **2004**, *126*, 4538–4539. (b) Lu, C. C.; Saouma, C. T.; Day, M. W.; Peters, J. C. *J. Am. Chem. Soc.* **2007**, *129*, 4–5.
(24) Brown, S. D.; Mehn, M. P.; Peters, J. C. *J. Am. Chem. Soc.* **2005**, *127*, 13146–13147.
(25) (a) Ohki, Y.; Suzuki, H. *Angew. Chem., Int. Ed. Engl.* **2000**, *39*, 3120–3122. (b) Nowik, I.; Herber, R. H. *J. Phys. Chem. Solids* **2003**, *64*, 313–317.
(26) (a) Koutmos, M.; Coucouvanis, D. *Inorg. Chem.* **2004**, *43*, 6508–6510. (b) Koutmos, M.; Georgakaki, I. P.; Coucouvanis, D. *Inorg. Chem.* **2006**, *45*, 3648–3656.
(27) Sadique, A. R.; Gregory, E. A.; Brennessel, W. W.; Holland, P. L. *J. Am. Chem. Soc.* **2007**, *129*, 8112–8121.
(28) Yu, Y.; Brennessel, W. W.; Holland, P. L. *Organometallics* **2007**, *26*, 3217–3226.
(29) (a) Vela, J.; Stoian, S.; Flaschenriem, C. J.; Münck, E.; Holland, P. L. *J. Am. Chem. Soc.* **2004**, *126*, 4522–4523. (b) Eckert, N. A.; Stoian, S.; Smith, J. M.; Bominaar, E. L.; Münck, E.; Holland, P. L. *J. Am. Chem. Soc.* **2005**, *127*, 9344–9345.
(30) Differences between the behaviors of **1a** and **1b** are attributed to steric effects : Vela, J.; Vaddadi, S.; Cundari, T. R.; Smith, J. M.; Gregory, E. A.; Lachicotte, R. J.; Flaschenriem, C. J.; Holland, P. L. *Organometallics* **2004**, *23*, 5226–5239.
(31) (a) Li, J.-G.; Burgess, B. K.; Corbin, J. L. *Biochemistry* **1982**, *21*, 4393–4402. (b) Rubinson, J. F.; Corbin, J. L.; Burgess, B. K. *Biochemistry* **1983**, *22*, 6260–6268. (c) Lowe, D. J.; Fisher, K.; Thorneley, R. N. F.; Vaughn, S.; Burgess, B. K. *Biochemistry* **1989**, *28*, 8460–8466. (d) Miller, R. W.; Eady, R. R. *Biochim. Biophys. Acta* **1988**, *952*, 290–296.

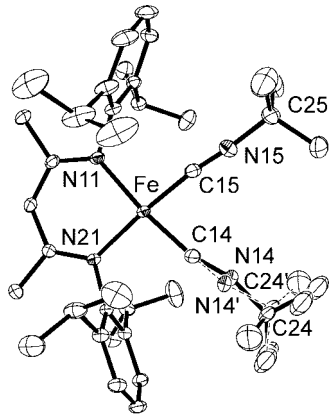

Figure 3. Molecular structure of $L^{Me}Fe(CN^tBu)_2$ (**2a**), showing 50% thermal ellipsoids. There is 50:50 disorder in the position of one isocyanide ligand. Selected bond distances (Å) and angles (°): Fe−C14 1.817(1), Fe−C15 1.821(1), C14−N14 1.222(9), C14−N14′ 1.153(9), C15−N15 1.173(2), C14−N14−C24 148.3(7), C14−N14′–C24′ 164.0(7), C15−N15−C25 170.1(2).

^{1}H NMR and X-band EPR spectra of samples prepared in this way were identical to the spectra of material generated from **1a**.

Solutions of the isocyanide complex **2a** decompose over several hours in solution at room temperature, making the results of bulk magnetic studies unreliable, but EPR spectra of frozen mixtures of $L^{Me}FeNNFeL^{Me}$ and 1−4 equiv of ^{t}BuNC in toluene show a rhombic signal with $g = 2.45, 2.24, 1.98$, suggesting that **2a** has an $S = {}^1/_2$ ground state.[32,33] In the solid-state infrared spectrum of **2a**, four stretching bands are observed at 2122, 2050, 1969, and 1948 cm^{-1}. Some bands almost certainly derive from decomposition products, because bands at 2050, 1969, and 1948 cm^{-1} are observed in the IR spectrum of a sample from allowing **2a** to completely decompose. Therefore, only the peak at 2122 cm^{-1} can be assigned confidently as a C≡N stretching vibration of **2a**. Computations (see below for details) predict the second stretching vibration at 2050 cm^{-1} after correction for anharmonicity, so it is possible that the peak at 2050 cm^{-1} derives from **2a** as well as a decomposition product.

The product has also been characterized by X-ray diffraction of a crystal grown at low temperature. The solid-state structure of **2a** is illustrated in Figure 3. The iron atom has a square planar geometry, with the sum of angles 360.4(5)°. The two isocyanides are not identical: one CNC angle is almost linear (170.1(2)°) while the other is bent. The bent isocyanide ligand is disordered; two positions of the ^{t}Bu group were observed, and the ratio of components is exactly 50:50 owing to the presence of a crystallographic inversion center. Both refined ligand positions show bent isocyanide ligands (CNC angles of 164.0(7)° and 148.3(7)°). The refinement model required that geometrical restraints be placed on the N^{t}Bu portions of the two ligand disorder components, specifically that the N−C(^{t}Bu) bond lengths and angles in both components be similar. The result is a disorder model that confirms the CNC bending, but that should be used with caution with regard to the exact values of the angles.

The ambiguous spectroscopic and crystallographic data left unanswered questions about **2a**. Therefore, hybrid quantum mechanics/molecular mechanics (QM/MM) computations were performed to study complete models of **2a**. The optimized geometry of the doublet state ($E_{relative} = 0$) is square planar about iron, but the higher energy quartet state ($E_{relative} = 3.9$ kcal/mol) has a tetrahedral coordination geometry upon QM/MM geometry optimization. The calculated metrical parameters for doublet $L^{Me}Fe(CN^tBu)_2$ (compared to experimental ones in parentheses) are Fe−C = 1.83 Å (1.82 Å); CN = 1.18 Å (1.15, 1.17, 1.22 Å). Both the lower calculated energy and the geometrical similarity to the experimental structure support the contention that **2a** has an $S = {}^1/_2$ ground state.

The computations also address the unusual difference between the CNC angles of the two isocyanide ligands (we denote the difference between these CNC angles as θ). The optimized geometry had CNC angles of 171° (close to the crystallographic angle of 170°) and 162° (between the observed 164° and 148° disorder components). A search of the Cambridge Structural Database for neutral, monometallic complexes with at least two ^{t}BuNC ligands indicated that the average θ is 6.9 ± 10.1° (170 examples) with a median value of 2.9°.[34] Hence, our computed value of $\theta = 9°$, while somewhat large, is not outside experimental norms. Computations indicate that bending the CNC angle from 180° to 150° requires 4 kcal/mol in free ^{t}BuNC and only 0.4 kcal/mol in the QM/MM model of **2a**.[35] Considering the softness of this bending distortion, it is not surprising that the isocyanide is unusually flexible and can exist in multiple geometries in the solid state.

In the next section, we turn to reactions with nitriles, mimics of cyanide with substituents on the carbon. Scheme 1 shows the reduction products obtained from CH_3CN and ^{t}BuCN. Heating **1a** with 2 equiv of CH_3CN in toluene at 45 °C for

Scheme 1

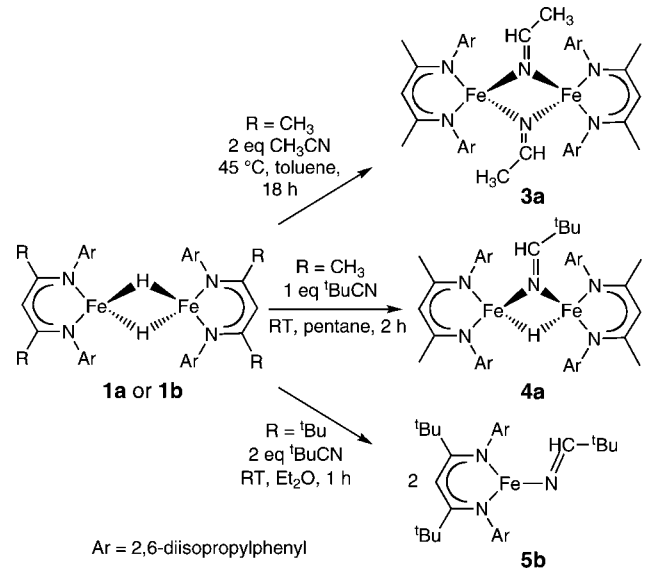

(32) The X-band EPR spectrum of the solutions are consistent with a mixture of at least two compounds. In addition to the signal described in the text, there is a less rhombic signal with $g = 2.08, 2.06, 2.00$ (see Supporting Information). These signals are almost identical to those previously identified as $L^{tBu}Fe(CO)_2$[33] and $L^{tBu}Fe(CO)_3$,[47] supporting the assignment of the more rhombic signal as $L^{Me}Fe(CN^tBu)_2$ and the less rhombic signal as $L^{Me}Fe(CN^tBu)_3$. The solution behavior of iron(I) isocyanide complexes will be described at length in a future publication.

(33) Sadique, A. R.; Brennessel, W. W.; Holland, P. L. *Inorg. Chem.* **2008**, *47*, 784–786.

(34) Cambridge Structural Database, 2006 update: Allen, F. H. *Acta Crystallogr.* **2002**, *B58*, 380. We used only high-quality (i.e., $R <$ 10%) non-polymeric structures with no crystallographic disorder.

(35) Similarly soft bending potentials have been seen in metal-imido complexes: Cundari, T. R.; Russo, M. *J. Chem. Inf. Comput. Sci.* **2001**, *41*, 281−287.

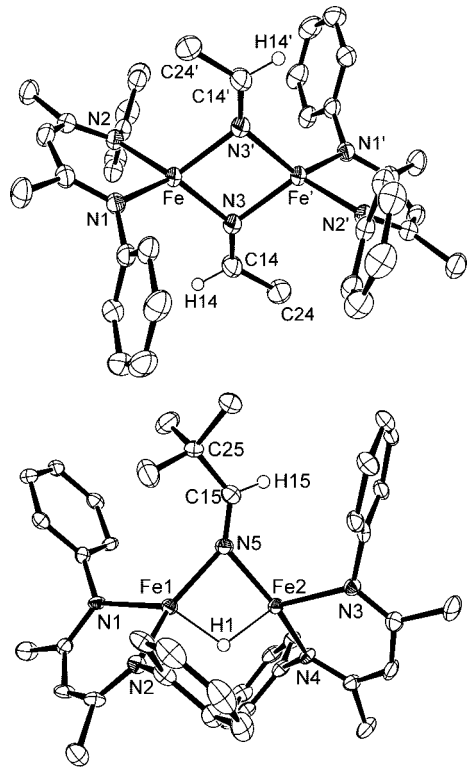

Figure 4. Molecular structures of **3a** (top) and **4a** (bottom), showing 50% thermal ellipsoids. The aryl isopropyl groups are omitted for clarity. Selected bond distances (Å) and angles (deg) for **3a**: Fe−N3, 2.041(2); Fe−N3′, 2.079(2); N3−C14, 1.258(2); Fe−N3−Fe′, 96.72(6); N3−C14−C24, 125.4 (2). For **4a**: Fe1−Fe2, 2.7816(8); Fe1−N5, 2.000(3); Fe2−N5, 2.016(3); Fe1−H1, 1.69(3); Fe2−H1, 1.67(3); N5−C15, 1.258(4); Fe1−N5−Fe2, 87.7(1); N5−C15−C25, 129.3(3).

18 h gives an orange-yellow precipitate in 88% yield. The X-ray crystal structure shows that the product is $L^{Me}Fe(\mu\text{-}N{=}CHCH_3)_2FeL^{Me}$ (**3a**) (Figure 4, top), with a crystallographic inversion center relating the two halves of the molecule. Each nitrile molecule has been reduced to a bridging $N{=}CHCH_3$ ligand with an N=C distance of 1.258(2) Å. The iron centers in **3a** have roughly tetrahedral geometries. The ^{1}H NMR spectrum of **3a** in toluene-d_8 has peaks from 50 to −40 ppm, and the number and integrations are consistent with the C_{2h} symmetry in the crystal structure.

When **1a** is treated with the bulkier nitrile ^{t}BuCN, brown $L^{Me}Fe(\mu\text{-}N{=}CH^tBu)(\mu\text{-}H)FeL^{Me}$ (**4a**) is obtained in 85% yield. The diiron complex incorporates only one equivalent of the nitrile, even in the presence of excess ^{t}BuCN. Addition across an N≡C bond has formed a bridging $N{=}CH^tBu$ ligand, while the other bridging hydride remains untouched. The crystal structure of **4a** (Figure 4, bottom) indicates that the large ^{t}Bu group pushes the two β-diketiminate ligands toward the bridging hydride, which significantly reduces the dihedral angle between the two β-diketiminate planes to around 81° in each of the two independent molecules in the crystal structure. This structural distortion makes the ^{1}H NMR spectrum more complicated than in **3a**. At ambient temperature, approximately 16 peaks are observed. Severe overlap between peaks has made attempts to assign peaks and measure the solution magnetic moment unsuccessful. At −20 °C, these ∼16 peaks split into ∼25 peaks, consistent with a reduction of symmetry from C_s (in a conformation like that in the crystal structure, but with the two β-diketiminate ligand planes coplanar on average) to C_1 (the symmetry in the solid state).

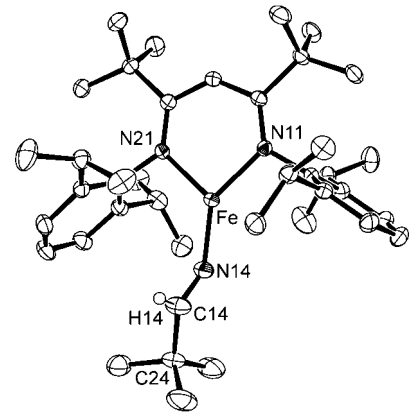

Figure 5. Molecular structure of **5b**, showing 50% thermal ellipsoids. Most hydrogen atoms have been omitted for clarity. Selected bond distances (Å) and angles (deg): Fe−N14, 1.857(2); Fe−N11, 1.977(2); Fe−N21, 1.966(2); N14−C14, 1.256(3); N11−Fe−N21, 94.69(6); N11−Fe−N14, 126.53(7); N21−Fe−N14, 138.70(7); Fe−N14−C14, 143.0(2).

Table 1. Comparisons among C≡N Insertion Products

property	3a	4a	5b
Symmetry from ^{1}H NMR at RT	C_{2h}	C_s	C_{2v}
Fe···Fe distance (Å)	3.0790(5)	2.7816(8)	N/A
N=C distance (Å)	1.258(2)	1.258(4)	1.256(3)
Dihedral angle between β-diketiminate ligand planes (deg)	0[a]	81.09(9), 80.6 (1)	N/A
N=C stretching frequency (cm^{-1})	1637	1629	1687
N−C−C angle in imide (deg)	125.4(2)	129.3(3)	127.2(3)
Fe−N(imide) distance (Å)	2.041(2), 2.079(2)	2.000(3), 2.016(3)	1.857(2)

[a] The two β-diketiminate ligand planes are related by a crystallographic inversion center.

Another kind of insertion product is observed when **1b** is treated with ^{t}BuCN. In this case, the orange product is monomeric $L^{tBu}Fe(N{=}CH^tBu)$ (**5b**) in 67% yield. The geometry around the iron atom is trigonal planar (Figure 5). A C=N double bond is indicated by the N14−C14 bond length of 1.256(3) Å and the C=N stretching band at 1687 cm^{-1}. The Fe−N(imide) bond length is 1.857(2) Å, substantially shorter than the Fe−N distances in the bridging imides of **3a** and **4a**.

Some triple bonds do not insert into the Fe−H bond. There is no evidence for thermal reaction of hydride complexes **1a** and **1b** with N_2: use of high pressures of dinitrogen (up to 800 psi at 60 °C) gave $L^{tBu}FeOFeL^{tBu}$, the product of reaction with moisture, as the only product observable by ^{1}H NMR spectroscopy.[29b] However, irradiation of each hydride complex under 1 atm of N_2 with a high-pressure mercury lamp yields quantitative conversion to $L^RFeNNFeL^R$ over the course of 18 h (**1a**) or 3 d (**1b**) as shown by ^{1}H NMR spectroscopy. These dinitrogen complexes have a formal oxidation state of +1 at each iron atom, and therefore result from reduction.[36] Therefore, it is possible to induce these hydride complexes to reductively eliminate H_2 and bind N_2, but this transformation requires photolysis.

(36) Loss of H_2 to give the dinitrogen complex is formally a reductive elimination, but the iron atoms in $L^{Me}FeNNFeL^{Me}$ are best described as $Fe^{2+}-N_2^{2-}-Fe^{2+}$ because of charge transfer to the N_2 ligand. See ref 19d.

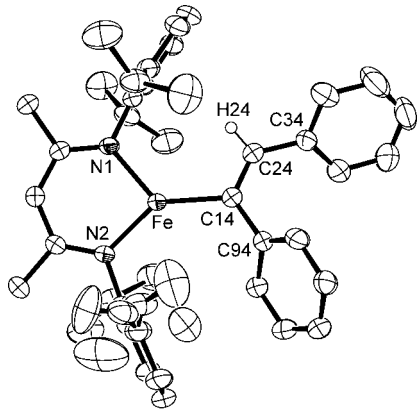

Figure 6. Molecular structure of $L^{Me}FeCPh{=}C(H)Ph$ (**6a**), showing 50% thermal ellipsoids. Selected bond distances (Å) and angles (deg): Fe−C14, 2.017(2); C14−C24, 1.347(2); C14−C24−C34, 129.0(2); C24−C14−C94, 121.6(2).

Reactions with C≡C Triple Bonds. Acetylene is the most commonly studied unnatural substrate of nitrogenases, and it is reduced to ethylene.[37] Mutant nitrogenase enzymes can also reduce longer-chain alkynes.[38,39] Here, we examine the reactivity of the low-coordinate iron hydride complexes with alkynes diphenylacetylene and 3-hexyne.

Complex **1a** inserts into the C–C triple bond in PhCCPh to form $L^{Me}FeC(Ph){=}C(H)Ph$ (**6a**) in 75% yield. This vinyl product is analogous to $L^{tBu}FeC(Et){=}C(H)Et$ (**6b**), which was previously reported from the reaction of **1b** with 3-hexyne.[20] Figure 6 presents the crystal structure of **6a**. The C−C distance (1.347(2) Å) and C−C−C angles (129.0(2)°, 121.6(2)°) in the vinyl ligand confirm that both carbons of the C=C double bond have sp^2 hybridization. The ^{1}H NMR spectrum of **6a** shows seven peaks for the β-diketiminate protons, indicating averaged C_{2v} symmetry from rapid rotation around the Fe−C14 bond on the NMR time scale.

Monitoring the reaction of **1a** with PhC≡CPh, or the reaction of **1b** with EtC≡CEt, shows no dependence of the reaction rate on [PhC≡CPh] (Table 2). Therefore, the rate laws are rate = k[**1**] with first-order rate constants $1.7(2) \times 10^{-3}$ s^{-1} (**1a**/PhCCPh at 31 °C) and $5.0(5) \times 10^{-4}$ s^{-1} (**1b**/EtCCEt at 15 °C). The first-order rate law is inconsistent with the interaction of alkyne with **1a** or **1b** during or prior to the rate-limiting step of the reaction. Two mechanistic possibilities consistent with the rate law are shown in Scheme 2. In pathway A, the opening of a single Fe−H bond is the rate determining step. We consider this Fe−H bond opening pathway to be more likely for the reaction of alkyne with **1a** because (1) there is no other evidence for any monomer form of **1a** by NMR or UV−vis spectroscopy; (2) in the reaction of **1a** with boranes, the rate law was first-order in [**1a**] and first-order in [BEt_3] but independent of the steric demands of the borane or iron complex.[28] These data were inconsistent with dissociation of **1a** into monomers (which predicts a half-order dependence on [**1a**]) and most consistent with single Fe−H opening, as in the bottom reaction pathway here. In pathway B, dimer cleavage is the rate determining step,

Scheme 2

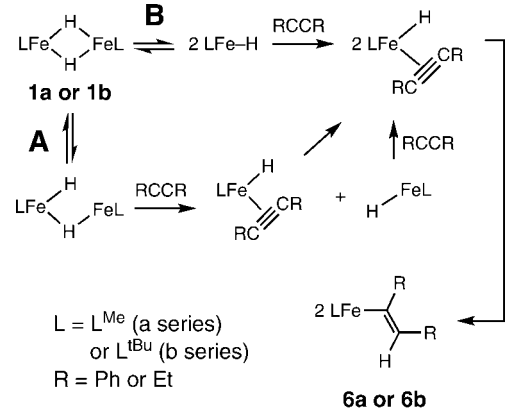

Table 2. Effect of [PhC≡CPh] on the Rate of Reaction with **1a** To Give **6a**[a]

[PhC≡CPh] (mM)	[PhC≡CPh]/[**1a**]	k_{obs} (s^{-1})
184	10.5	$1.7(1) \times 10^{-3}$
362	20.6	$1.6(1) \times 10^{-3}$
725	41.2	$1.7(2) \times 10^{-3}$

[a] [**1a**] = 17.6 mM in C_6D_6 at 30.8 °C. Details of the reaction of **1b** with 3-hexyne are given in ref 20.

as proposed for the reaction of **1b** with 3-hexyne.[20] This pathway is reasonable for **1b**, because the monomer is rapidly accessed at room temperature (see earlier). The rate of the reaction is consistent with the rapid equilibrium of monomer and dimer observed previously.[20] So, although the evidence is not definitive, the kinetic data here and elsewhere are most indicative of the pathway A in the reactions of alkynes with **1a**, but pathway B for alkyne reactions with **1b**. This difference is consistent with the greater steric demands of the diketiminate ligands in **1b** than **1a**.

Reactions with C=C Bonds. We previously reported that $L^{Me}Fe(alkyl)$ complexes with β-hydrogens can act as sources of transient hydride species $L^{Me}Fe(H)(alkene)$. These react with alkenes to give insertion products, and complexes $L^{Me}FeR'$ (R′ = ethyl, 1-propyl, 2-propyl, 1-butyl, 2-butyl, cyclohexyl, 2-phenethyl) were fully characterized.[30] We have also characterized numerous alkyl complexes of iron with the larger L^{tBu} ligand.[40] With isolated iron hydride complexes in hand, we verified that the addition of alkenes to isolated **1a** or **1b** gives alkyl complexes of the same type through [1,2] addition across the double bond. For example, reaction of **1a** with 1-hexene quantitatively gives a 1-hexyliron complex, as judged by ^{1}H NMR spectroscopy. It is worth noting that the transient iron hydride $L^{Me}Fe(H)(alkene)$ also adds across the C=N bonds of imines (forming $L^{Me}FeNR'CHR_2$ from $R_2C{=}NR'$) and the C=O bonds of ketones (forming $L^{Me}FeOCHR_2$ from $R_2C{=}O$).[30] Because these reactions have already been characterized starting from the alkyl complexes,[30] the reactions with isolated hydride complexes were not investigated further.

Reactions with Azides. The azide ion (N_3^-) is transformed by nitrogenase into N_2, NH_3, and N_2H_4.[40] Here, substituted azides AdN_3 (Ad = 1-adamantyl) and Me_3SiN_3 are used as

(37) Yates, M. G. "Molybdenum-Dependent Nitrogen Fixation". In *Biological Nitrogen Fixation;* Stacey, G., Burris, R. H., Evans, H. J., Eds.; Chapman & Hall: New York, 1992; pp 685−735 .
(38) Dos Santos, P. C.; Igarashi, R. Y.; Lee, H.-I.; Hoffman, B. M.; Seefeldt, L. C.; Dean, D. R. *Acc. Chem. Res.* **2005**, *38*, 208–214.
(39) Lee, H.-I.; Igarashi, R. Y.; Laryukhin, M.; Doan, P. E.; Dos Santos, P. C.; Dean, D. R.; Seefeldt, L. C.; Hoffman, B. M. *J. Am. Chem. Soc.* **2004**, *126*, 9563–9569.
(40) Smith, J. M.; Lachicotte, R. J.; Holland, P. L. *Organometallics* **2002**, *21*, 4808–4814.
(41) (a) Schöllhorn, R.; Burris, R. H. *Proc. Natl. Acad. Sci. U.S.A.* **1967**, *57*, 1317–1323. (b) Dilworth, M. J.; Thorneley, R. N. F. *Biochem. J.* **1981**, *193*, 971–983.

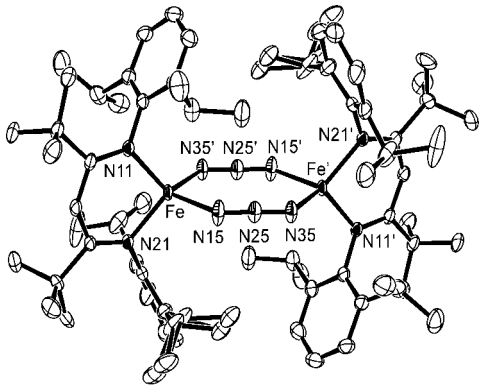

Figure 7. Molecular structure of $L^{tBu}Fe(\mu\text{-}N_3)_2FeL^{tBu}$ (**7b**), showing 50% thermal ellipsoids. Selected bond distances (Å) and angles (deg): Fe−N15, 2.061(1); Fe−N35, 2.025(1); Fe−N11, 1.988 (1); Fe−N21, 1.989(1); N15−N25, 1.167(2); N25−N35, 1.176(2); N11−Fe−N21, 97.10(4); N15−Fe−N35, 95.17(4); N15−N25−N35, 177.0(1).

Scheme 3

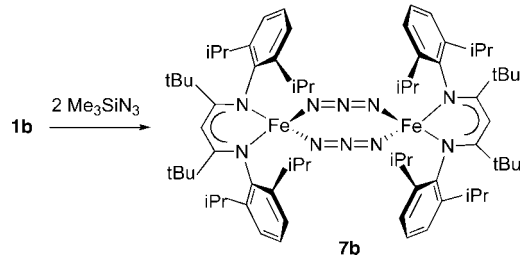

models. The reactions of organic azides with transition-metal complexes have been reviewed recently.[42]

Reactions of complex **1a** with Me_3SiN_3 give mixtures, as judged from ^1H NMR spectra. However, complex **1b**, when treated with 2 equiv of trimethylsilyl azide in diethyl ether, gives a dimeric azide complex, $L^{tBu}Fe(\mu\text{-}N_3)_2FeL^{tBu}$ (**7b**) in 79% yield (Scheme 3). Compound **7b** can be prepared independently by reacting $L^{tBu}FeCl$[43] with sodium azide.

The X-ray crystal structure of **7b** (Figure 7) shows that the compound is dinuclear in the solid state with an Fe···Fe distance of 5.0966(4) Å. Each iron atom is coordinated to two azide ions, which bridge the iron atoms in a $\mu_{1,3}$-end-to-end fashion with inequivalent iron−nitrogen bond lengths of 2.061(1) and 2.025(1) Å. The eight atoms of the Fe_2N_6 core are coplanar, in contrast to the only other crystallographically characterized end-to-end bridged iron azide complex, $[(PhBP_3)Fe(\mu\text{-}1,3\text{-}N_3)]_2$ ($PhBP_3$ = $[PhB(CH_2PPh_2)_3]^-$), which has a chair conformation.[44] The dihedral angle between the Fe_2N_6 plane and the Fe_2N_2 (diketiminate) plane is 87.41(4)°. The azide ligands are almost linear (N−N−N angle of 177.0(1)°) and the N−N bond lengths within the azide groups (1.167(2), 1.176(2) Å) show double bond character similar to N−N distances in other bridging azide complexes.[34] The solid-state IR spectrum of **7b** shows characteristic azide bands at 2129 and 2081 cm^{-1}.[45]

$^{29}Si\{^1H\}$ NMR analysis of the volatile products in the reaction mixture revealed a resonance at −22 ppm for $Me_3SiSiMe_3$, but none for Me_3SiH. The production of $Me_3SiSiMe_3$ implies that two hydrogen atoms were lost. However, H_2 was not detected in the headspace by gas chromatography, so the fate of the hydrogen atoms is unclear. The coupling of two trimethylsilyl units strongly implies the intermediacy of $Me_3Si\bullet$ radicals. These in turn might derive from the attack of an iron radical on trimethylsilyl azide.[46] To test this idea, the iron(I) sources $L^{tBu}FeNNFeL^{tBu}$ [47] and $L^{tBu}FeClK(solvent)_x$[47] were each treated separately with Me_3SiN_3. In each case, $[L^{tBu}FeN_3]_2$ was formed. Therefore, iron(I) species of this type are reasonable intermediates that could be formed by homolysis of Fe−H bonds. Homolysis of Fe−H bonds does not occur spontaneously in **1b** at room temperature, and therefore we infer that coordination of Me_3SiN_3 weakens the Fe−H bond and brings about Fe−H homolysis.

Compound **1b** undergoes an insertion reaction with AdN_3 to give 67% yield of a triazenido complex, $L^{tBu}Fe(\eta^2\text{-}HNNNAd)$ (**8b**), which is shown in Scheme 4 and Figure 8. The bidentate triazenide and β-diketiminate ligands are perpendicular to each other, which gives a distorted tetrahedral geometry around the metal center. The presence of an N−H band in **8b** is confirmed by the observation of a weak bond at ν_{N-H} at 3371 cm^{-1} in the infrared spectrum. The ^1H NMR spectrum of **8b** is indicative of C_{2v} local symmetry at temperatures from room temperature to −75 °C, despite the C_s-idealized symmetry of the molecule in the solid state (each face of the diketiminate ligand should be inequivalent). This observation implies that there is rapid exchange between the two possible orientations of the triazenido ligand. Considering the stability of three-coordinate complexes $L^{tBu}FeX$ and the large size of the

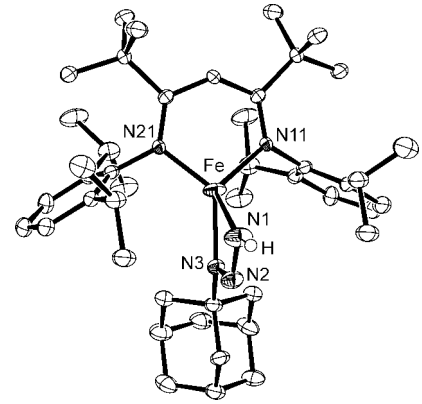

Figure 8. Molecular structure of triazenido complex **8b**, showing 50% thermal ellipsoids. Selected bond distances (Å) and angles (deg): Fe−N1, 2.081(2); Fe−N3, 2.078(2); Fe−N11, 1.878(4); Fe−N21, 2.117(4); N1−N2, 1.310(3); N2−N3, 1.285(2); N3−C1, 1.463(7); N11−Fe−N21, 98.32(9); N1−Fe−N3, 60.46(7); N1−N2−N3, 107.6(2).

Scheme 4

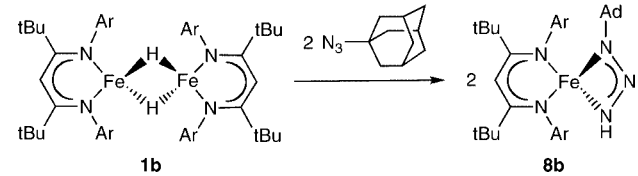

(42) Cenini, S.; Gallo, E.; Caselli, A.; Ragaini, F.; Fantauzzi, S.; Piangiolino, C. *Coord. Chem. Rev.* **2006**, *250*, 1234–1253.
(43) (a) Smith, J. M.; Lachicotte, R. J.; Holland, P. L. *Chem. Commun.* **2001**, 1542–1543. (b) Smith, J. M.; Lachicotte, R. J.; Holland, P. L. *Organometallics* **2002**, *21*, 4808–4814.
(44) Brown, S. D.; Peters, J. C. *J. Am. Chem. Soc.* **2005**, *127*, 1913–1923.
(45) These are similar to the bands observed in literature compounds: Cortes, R.; Drillon, M.; Solans, X.; Lezama, L.; Rojo, T. *Inorg. Chem.* **1997**, *36*, 677–683.
(46) The homolytic Si−N bond energy in Me_3SiN_3 is 76 kcal/mol: Adeosun, S. O. *Inorg. Nucl. Chem. Lett.* **1976**, *12*, 301–305.
(47) Smith, J. M.; Sadique, A. R.; Cundari, T. R.; Rodgers, K. R.; Lukat-Rodgers, G.; Lachicotte, R. J.; Flaschenriem, C. J.; Vela, J.; Holland, P. L. *J. Am. Chem. Soc.* **2006**, *128*, 756–769.

adamantyl group, it seems most reasonable to attribute this behavior to a rapid, reversible isomerization of the triazenido ligand from η^2 to η^1, followed by rotation and recoordination.

Although disubstituted triazenido complexes are well-known in the literature, there are few examples of triazenido complexes bearing H as one substituent; they come from insertion of azide into a hydride complex,[48,49] and from protonation of an azide complex.[50,51] Free H_2NNNR compounds are extremely unstable with respect to loss of N_2. Although compound **8b** is thermally stable for hours in solution at room temperature, it eventually decomposes to the Fe(II) amido complex L^{tBu}FeNHAd with loss of N_2. (For identification, L^{tBu}FeNHAd was synthesized independently from L^{tBu}FeCl and LiNHAd by analogy to other known iron(II) amido complexes.[52]) Quantitative transformation from triazenido to amido was observed by ^{1}H NMR spectroscopy after heating a sample of **8b** in C_6D_6 at 80 °C for 5 h.

Reactions with N═N Double Bonds. Diazene (HN═NH) is a possible intermediate of N_2 fixation by nitrogenase. Consistent with this idea, both HN═NH and CH_3N═NH are nitrogenase substrates,[53] and CH_3N═NCH_3 is reduced by nitrogenase to give ammonia, methane, and methylamine.[54] Very recently, hydrazine (N_2H_4), methyldiazene (HN═NCH_3) and N_2 derived nitrogenase intermediates have been freeze-trapped.[55] Free diazenes bearing hydrogen substituents are extremely difficult to handle, because they decompose in seconds or minutes. As an alternative approach, we have used the stable diazenes azobenzene (PhN═NPh) and benzo[*c*]cinnoline.

We recently reported a detailed study of the reaction of **1b** with PhN═NPh, which leads first to the [1,2]-addition product L^{tBu}FeNPhNHPh, and subsequently to the amido complex L^{tBu}FeNHPh.[27] Mechanistic studies were most consistent with a radical chain mechanism, mediated by an iron(I) carrier.[27] Reaction of the smaller **1a** with PhN═NPh at ambient temperature gives a mixture of products as judged by the ^{1}H NMR spectrum. It has not been possible to purify and isolate these compounds, but they may be tentatively assigned as L^{Me}FeNPhNHPh and L^{Me}FeNHPh on the basis of the similarity of their ^{1}H NMR spectra with the L^{tBu} analogues.[27] Longer reaction time or heating does not drive the reaction mixture to L^{Me}FeNHPh. Instead decomposition occurs, probably due to the instability of L^{Me}FeNHPh.[52]

We also investigated the reaction of **1a** with 2 equiv of benzo[*c*]cinnoline, which gave 90% conversion to deep green **9a**. The detection of 1.07(3) equiv of H_2 by GC is consistent with the reaction stoichiometry shown in Scheme 5. In this case, there is no addition across the N═N double bond; rather, H_2 is lost and the benzo[*c*]cinnoline coordinates to iron. Alternatively,

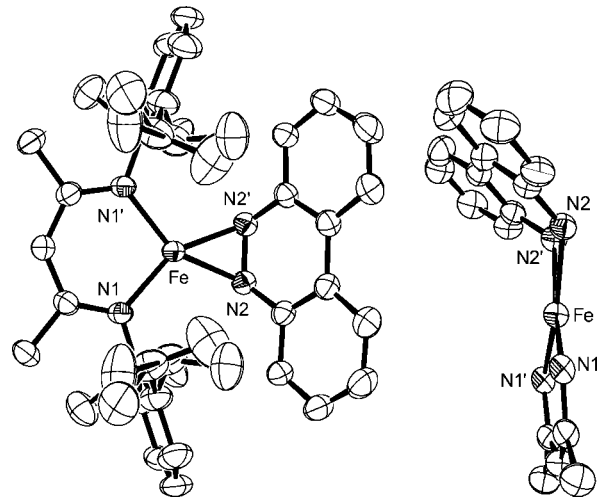

Figure 9. Two views of the molecular structure of **9a**, showing 50% thermal ellipsoids. In the picture on the right, aryl groups are removed for clarity. Selected bond distances (Å) and angles (deg): Fe−N2, 1.967(1); N2−N2′, 1.385(2); N2−Fe−N2′, 41.22(7). The dihedral angle between the β-diketiminate FeNCCNFe plane and the benzo[*c*]cinnoline plane is 55.35(5)°.

Scheme 5

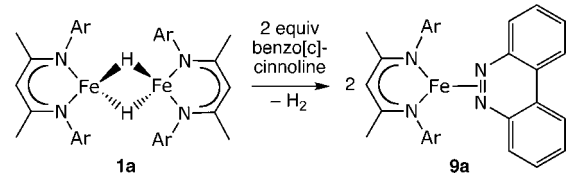

9a could be isolated in 91% yield from the reaction of L^{Me}FeNNFeL^{Me} and benzo[*c*]cinnoline.

The crystal structure of **9a** (Figure 9) shows that benzo[*c*]cinnoline binds face-on to iron(I) through the N═N π-bond, and the N−N distance is 1.138(5) Å. The dihedral angle between the benzo[*c*]cinnoline and the β-diketiminate ligand is 55.35(5)°. A side-on interaction between iron and an N═N double bond has been crystallographically confirmed in only two other compounds. In [Fe(NO)$_2${$PPh_2CH_2CH_2PPh_2$NNAr}][PF_6], the diazene (N═N 1.403(5)) is constrained to bind using a bidentate phosphine;[56] and our recently reported L^{tBu}Fe(PhNNPh) has an N═N distance of 1.398(2) Å.[27]

The peaks in the ^{1}H NMR spectra of C_6D_6 solutions of **9a** are unusually broad. Mixing different ratios of **1a** and benzo[*c*]cinnoline indicates that the broadness of the peaks increases with a greater concentration of benzo[*c*]cinnoline, and becomes substantially sharper at a 1:1 ratio of **1a** to benzo[*c*]cinnoline (see Supporting Information for spectra). This behavior suggests that free and bound benzo[*c*]cinnoline exchange at a rate near the NMR time scale (milliseconds). The spectra are substantially sharper in C_6D_{12}, indicating that exchange of the aromatic with C_6D_6 is part of this process. We have previously characterized L^{Me}Fe(η^6–C_6H_6), in which the benzene ligand is bound relatively weakly (it is displaced rapidly by phosphines, alkenes, and alkynes).[57] Since benzene competes effectively with benzo[*c*]cinnoline as a ligand, it shows that the heteroaromatic π-ligand is bound weakly as well.

(48) (a) Burgess, K.; Johnson, B. F. G.; Lewis, J.; Raithby, P. R. *J. Organomet. Chem.* **1982**, *224*, C40–C44. (b) Johnson, B. F. G.; Lewis, J.; Raithby, P. R.; Sankey, S. W. *J. Organomet. Chem.* **1982**, *228*, 135–138.
(49) Hillhouse, G. L.; Bercaw, J. E. *Organometallics* **1982**, *1*, 1025–1029.
(50) Wang, Z. X.; Miao, S. B.; Zhou, Z. Y.; Zhou, X. G. *J. Organomet. Chem.* **2000**, *601*, 87–92.
(51) Hillhouse, G. L.; Haymore, B. L. *J. Organomet. Chem.* **1978**, *162*, C23.
(52) Eckert, N. A.; Smith, J. M.; Lachicotte, R. J.; Holland, P. L. *Inorg. Chem.* **2004**, *43*, 3306–3321.
(53) Barney, B. M.; Lukoyanov, D.; Yang, T.-C.; Dean, D. R.; Hoffman, B. M.; Seefeld, L. C. *Proc. Natl. Acad. Sci. U.S.A.* **2006**, *103*, 17113–17118.
(54) McKenna, C. E.; Simeonov, A. M.; Eran, H.; Bravo-Leerahhandh, M. *Biochemistry* **1996**, *35*, 4502–4514.
(55) Barney, B. M.; Yang, T.-C.; Igarashi, R. Y.; Dos Santos, P. C.; Laryukhin, M.; Lee, H.-I.; Hoffman, B. M.; Dean, D. R.; Seefeldt, L. C. *J. Am. Chem. Soc.* **2005**, *127*, 14960–14961.
(56) Atkinson, F. L.; Connelly, N. G.; Crossley, J. G.; Orpen, A. G. *J. Chem. Soc., Dalton Trans.* **1994**, 1161–1162.
(57) Yu, Y.; Smith, J. M.; Flaschenriem, C. J.; Holland, P. L. *Inorg. Chem.* **2006**, *45*, 5742–5751.

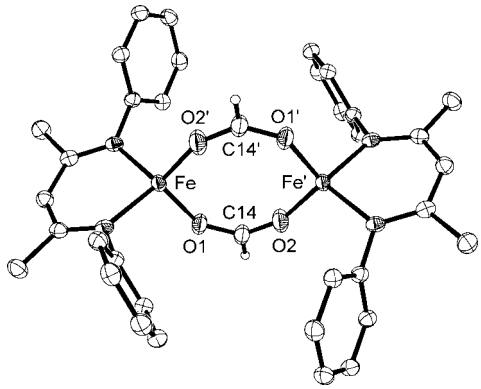

Figure 10. Molecular structure of $L^{Me}Fe(\mu\text{-}OCHO)_2FeL^{Me}$ (**10a**) showing 50% thermal ellipsoids. Isopropyl groups on the aryl rings are omitted for clarity. The structure of **10b** is similar and is shown in the Supporting Information. Selected bond distances (Å) and angles (deg) for **10a**: Fe−O, 1.978(2), 2.006(2); C−O, 1.245(3), 1.246(3); O−Fe−O, 115.57(7); O−C−O, 127.9(2). For **10b**: Fe−O, 1.967(1), 1.994(1); C−O 1.248(2), 1.245(2); O−Fe−O, 106.98(6); O−C−O, 128.2(2).

Reactions with Carbon Dioxide and Carbodiimide. After azide, CO_2 is another heterocumulene that is a substrate of nitrogenase. Seefeldt and co-workers have shown that CO_2 is slowly reduced to CO by the nitrogenase enzyme.[58]

Complexes **1a** and **1b** each react with 2 equiv of carbon dioxide at room temperature, generating yellow solids that are formulated as formate-bridging diiron complexes (**10a**, **10b**) based on X-ray crystallography (Figure 10). Only a few crystallographically characterized η^2-formato bridging iron complexes have been reported in the literature. These complexes were synthesized from iron formate, $Fe(O_2CH)_2 \cdot 2H_2O$,[59] reaction of iron metal and formic acid,[60] or $Fe(ClO_4) \cdot 10H_2O$ with NaO_2CH.[61] Reactions of CO_2 with iron hydride complexes are uncommon.[61]

The formate-bridged diiron complexes are insoluble in pentane, and only somewhat soluble in aromatic solvents, a problem that was especially severe for **10b**. The solution magnetic moment of **10a** is 8.8(2) μ_B, consistent with two nearly uncoupled high-spin iron(II) ions, and **10b** was too insoluble to derive a reliable value. The ^{1}H NMR spectrum of **10a** at room temperature has six peaks with chemical shifts that range from 18 ppm to −60 ppm, suggesting idealized D_{2h} symmetry. Although this observation is consistent with either monomer or dimer in solution, no decoalescence is seen in the ^{1}H NMR spectrum of **10a** in toluene from −35 to 120 °C, indicating that the crystallographically observed dimer is the most likely solution species. In **10b**, the ^{1}H NMR spectrum at 85 °C has only seven peaks that integrate as expected for a fully symmetric diketiminate ligand, and the chemical shifts are similar to those in **10a**. Interestingly, new peaks appear at lower temperatures.

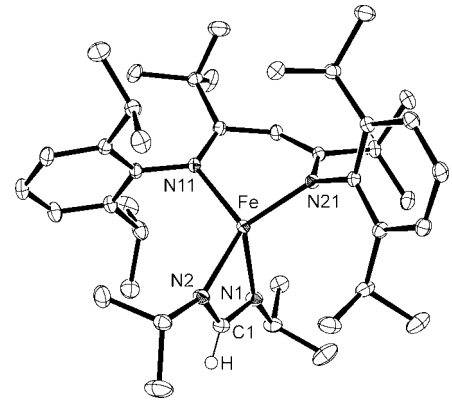

Figure 11. Molecular structure of **11b**, showing 50% thermal ellipsoids. Selected bond distances (Å) and angles (deg): Fe−N1, 2.1358(9); Fe−N2, 2.0675(8); Fe−N11, 2.0663(8); Fe−N21, 1.9908(8); N1−C1, 1.318 (1); N2−C1, 1.323(1); N1−Fe−N2, 64.50(3); N11−Fe−N21, 97.44(3); N1−C1−N2, 116.27(8).

These peaks are consistent with splitting of a isopropyl methine and one isopropyl methyl resonance, which correspond to the protons closest to one another in the dimer. Unfortunately, the poor solubility of **10b**, especially at low temperature, prevents us from fully characterizing this phenomenon. The available data are consistent with either a monomer−dimer equilibrium, or a change from slow to rapid flipping of the diketiminate planes to each side of a dimer (change from C_{2h} to effective D_{2h} point group symmetry).

To overcome the issues caused by the low solubility of these products, we investigated the analogous reaction of diisopropyl carbodiimide (^{i}PrN═C═N^{i}Pr) with **1b**. This reaction proceeded rapidly and quantitatively at room temperature to give the formamidinate complex $L^{tBu}Fe(^i\text{PrNCHN}^i\text{Pr})$ (**11b**) in 89% yield. This compound is monomeric, in contrast to the dimeric formate complexes derived from CO_2, a result that is most reasonably attributed to the steric hindrance of the isopropyl groups on the carbodiimide. In the solid state structure of **11b** (Figure 11) both the diketiminate ligand and the formamidinate ligand are coordinated in an η^2 fashion to the Fe atom, giving a distorted tetrahedral geometry around the metal center. The N−Fe−N bite angle of each ligand is typical.[34]

Reactions with Brønsted Acids. As described above, EPR investigations suggest that an FeMoco species with two hydrides can lose *two* equivalents of H_2 to return to the hydride-free resting state.[6] This suggests that some low-coordinate iron hydride species could be protonated by nearby Brønsted acids to give H_2. To investigate the susceptibility of synthetic Fe−H compounds to protonation of the hydride, we explored the reactions of **1a** and **1b** with weak acids.

In the presence of excess water, the low-coordinate iron hydride complexes decompose to intractable mixtures that contain free β-diketimine, suggesting that the acid protonates the α position of the β-diketiminate ligand. Reaction with smaller amounts of water often gives mixtures as well. In a few cases, using solutions of H_2O in tetrahydrofuran gives mixtures in which one compound predominates, enabling isolation. For example, we reported that addition of 1 equiv of H_2O to **1b** (0.5 equiv per iron) gives the unique oxodiiron(II) complex $L^{tBu}FeOFeL^{tBu}$ in 71% yield.[29b] In another reaction, the addition of 2 equiv of water to **1a** gives a green iron complex, $L^{Me}Fe(\mu\text{-}OH)_2FeL^{Me}$ (**12a**) in 67% yield (Scheme 6).

The solid state structure of **12a** (Figure 12) has pseudo-D_{2h} symmetry, and half of the molecule is related to the other half-

(58) Seefeldt, L. C.; Rasche, M. E.; Ensign, S. A. *Biochemistry* **1995**, *34*, 5382–5389.
(59) (a) Tolman, W. B.; Bino, A.; Lippard, S. J. *J. Am. Chem. Soc.* **1989**, *111*, 8522–8523. (b) Tolman, W. B.; Liu, S.; Bentsen, J. G.; Lippard, S. J. *J. Am. Chem. Soc.* **1991**, *113*, 152–164. (c) Sessler, J. L.; Hugdahl, J. D.; Lynch, V.; Davis, B. *Inorg. Chem.* **1991**, *30*, 334–336.
(60) Overgaard, J.; Rentschler, E.; Timco, G. A.; Gerbeleu, N. V.; Arion, V.; Bousseksou, A.; Tuchagues, J. P.; Larsen, F. K. *J. Chem. Soc., Dalton Trans.* **2002**, 2981–2986.
(61) Armstrong, W. H.; Spool, A.; Papaefthymiou, G. C.; Frankel, R. B.; Lippard, S. J. *J. Am. Chem. Soc.* **1984**, *106*, 3653–3667.
(62) (a) Field, L. D.; Lawrenz, E. T.; Shaw, W. J.; Turner, P. *Inorg. Chem.* **2000**, *39*, 5632–5638. (b) Field, L. D.; Shaw, W. J.; Turner, P. *Chem. Commun.* **2002**, 46–47. (c) Lu, C. C.; Saouma, C. T.; Day, M. W.; Peters, J. C. *J. Am. Chem. Soc.* **2007**, *129*, 4–5.

Scheme 6

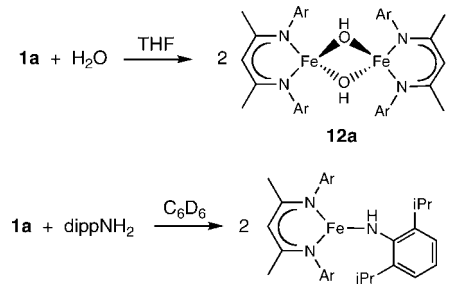

by a crystallographic inversion center. The metrical parameters compare well with other complexes containing a $Fe^2(\mu\text{-}OH)_2$ core.[34,63] Seven paramagnetically shifted peaks are observed in the ^{1}H NMR spectrum of **12a**, consistent with D_{2h} symmetry in solution. No peak clearly corresponding to the bridging OH is observed in the ^{1}H NMR spectrum, but O−H stretching vibrations are seen at 3709 and 3668 cm^{-1} in the IR spectrum. This binuclear complex has a solution magnetic moment of 7.5(1) μ_B per dimer, suggesting two uncoupled high-spin Fe(II) centers. Dihydrogen is observed by GC as another product of the reaction. Unfortunately, the THF and H_2O peaks overlap with the peak from the internal standard CH_4, which prevented quantitative measurement of the H_2 produced.

Finally, we tested 2,6-diisopropylaniline ($dippNH_2$), which has a similar acidity as water in organic solvents (the pK_a values in DMSO are 32 for H_2O and 30.6 for $PhNH_2$).[64] A mixture of **1a** and $dippNH_2$ in C_6D_6 quantitatively gives the iron amido complex L^{Me}FeNHdipp within a few hours (Scheme 6), as judged by ^{1}H NMR spectroscopy. Dihydrogen (1.6 equiv) is detected from the reaction, close to the 2 equiv expected. This iron amido complex was previously synthesized from $[L^{Me}FeCl]_2$.[52]

Discussion

Addition of Fe−H across a Multiple Bond. The low coordination number at the iron atoms in these hydride complexes enables reactions with many unsaturated organic compounds. Rapid [1,2] additions are seen with alkenes, alkynes, imines, ketones, nitriles, carbodiimides, and carbon dioxide. These reactions generally place the iron fragment on the more electronegative atom of the double bond, and the hydrogen on the less electronegative atom. These are not uncommon reactions of transition-metal hydride complexes,[1] but they appear to be quite rapid in this system relative to literature iron complexes of higher coordination number. For example, a mixture of *trans*-$[FeHCl(dppe)_2]$ and $TlBF_4$ reacts only with alkynes in which there is an ester functionality that can chelate to the metal.[65] The reactions of phosphine-supported octahedral iron hydrides with alkynes often give a variety of products, including acetylide and vinylidene complexes.[66] Known saturated iron hydride complexes do not react with alkenes[66] except cyclopropene.[67] Although there are not many literature examples of heterocumulenes (CO_2, CS_2, carbodiimides) reacting with iron hydrides, these reactions appear to be facile in one case.[68]

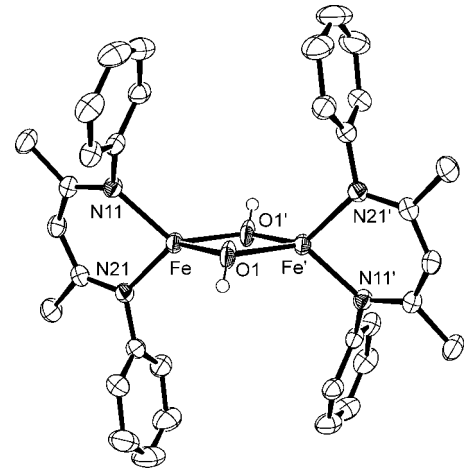

Figure 12. Molecular structure of 12a, showing 50% thermal ellipsoids. Isopropyl groups removed for clarity. Selected bond distances (Å) and angles (deg): Fe−O1, 2.082(3), 2.059(6); Fe−O1−Fe′, 98.7(2); O1−Fe−O1′, 81.3(2).

Cyanide compounds (nitriles) are not usually reactive toward insertion into the Fe−H bonds of iron−hydride complexes, aside from one example of insertion from a dinuclear iron−carbonyl complex.[68] Acetonitrile more typically coordinates to iron.[70] In the β-diketiminate complexes described here, the iron hydrides reduce RCN to a $RC(H)=N^-$ ligand under mild conditions. Interestingly, the outcome of the insertion reactions is dependent on the steric demands of the β-diketiminate ligand and the nitrile. With the bulkiest β-diketiminate (L^{tBu}) and nitrile (^{t}BuCN), the product is a monomeric complex. With the smallest β-diketiminate (L^{Me}) and nitrile (CH_3CN), the product is a dimer with two bridging imidoyl ligands. Finally, with ^{t}BuCN and the less bulky hydride complex, a single insertion occurs and the steric bulk prevents access of the second nitrile to the remaining bridging hydride.

The reaction of adamantyl azide with **1b** gives a triazenido complex that results from formal [1,1]-addition. A few late-metal alkyl complexes have been observed to give [1,1]-addition to azides.[70] The lone example of a triazenido ligand on iron is in a dinuclear iron−carbonyl complex, where the triazenide derives from protonation of an anionic azide complex.[71] To our knowledge, the only other reaction of an iron hydride complex with an azide involves the addition of sodium azide to L_2FeH_2

(63) Another coordinatively unsaturated bis(μ-hydroxo)diiron(II) complex has more acute angles at iron, presumably from steric clashes between bulky tris(pyrazolyl)borate ligands: Kisko, J. L.; Hascall, T.; Parkin, G. *J. Am. Chem. Soc.* **1998**, *120*, 10561−10562.

(64) pK_a values from http://www2.lsdiv.harvard.edu/labs/evans/pdf/evans_pKa_table.pdf; accessed April 7, 2008.

(65) Almeida, S. S. P.; Duarte, M. T.; Ribeiro, L. M. D.; Gormley, F.; Galvao, A. M.; Frausto Da Silva, J. J. R.; Pombeiro, A. J. L. *J. Organomet. Chem.* **1996**, *524*, 63–66.

(66) (a) Bianchini, C.; Meli, A.; Peruzzini, M.; Frediani, P.; Bohanna, C.; Esteruelas, M. A.; Oro, L. A. *Organometallics* **1992**, *11*, 138–145. (b) Hughes, D. L.; Leigh, G. J.; Jimenez-Tenorio, M.; Rowley, A. T. *J. Chem. Soc., Dalton Trans.* **1993**, 75–82.

(67) Hughes, D. L.; Leigh, G. J.; McMahon, C. N. *J. Chem. Soc., Dalton Trans.* **1999**, 909–914.

(68) (a) Bianco, V. D.; Doronzo, S.; Rossi, M. *J. Organomet. Chem.* **1972**, *35*, 337–339. (b) Matsubara, T.; Hirao, K. *Organometallics* **2001**, *20*, 5759–5768. (c) Field, L. D.; Lawrenz, E. T.; Shaw, W. J.; Turner, P. *Inorg. Chem.* **2000**, *39*, 5632–5638. (d) Field, L. D.; Shaw, W. J.; Turner, P. *Organometallics* **2001**, *20*, 3491–3499.

(69) Hogarth, G.; Lavender, M. H.; Shukri, K. *Organometallics* **1995**, *14*, 2325–2341.

(70) (a) Collman, J. P.; Finke, R. G.; Matlock, P. L.; Wahren, R.; Brauman, J. I. *J. Am. Chem. Soc.* **1976**, *98*, 4685–4687. (b) Albertin, G.; Antoniutti, S.; Lanfranchi, M.; Pelizzi, G.; Bordignon, E. *Inorg. Chem.* **1986**, *25*, 950–957.

(71) Chiu, K. W.; Wilkinson, G.; Thornton-Pett, M.; Hursthouse, M. B. *Polyhedron* **1984**, *3*, 79–85.

(72) Wang, Z. X.; Miao, S. B.; Zhou, Z. Y.; Zhou, X. G. *J. Organomet. Chem.* **2000**, *601*, 87–92.

(L = bidentate phosphine ligand) in methanol, which replaces the hydride ligand with azide.[73] A search of the CSD shows that $L^{tBu}Fe(HNNNAd)$ is the first structurally characterized complex of a triazenido ligand bearing a hydrogen atom.[34] Mechanistic and spectroscopic studies indicated the formation of hafnium, rhenium, and tungsten triazenido complexes from the reaction of azides with hydride species.[51,74] In the hafnium complex, mechanistic studies indicated that the $HNNN(aryl)^-$ ligand decomposes to $NH(aryl)^-$ through a shift of the hydrogen atom to the carbon-bound nitrogen atom, followed by extrusion of N_2. In the iron system studied here, a similar mechanism can explain the conversion of the triazenido complex to $L^{tBu}FeNHAd$.

Recent reports of other low-coordinate iron systems are also indicative of high reactivity, although hydride species were not isolable in these systems. For example, Chirik has used low-coordinate pyridinediimine−iron and α-diimine−iron complexes as precatalysts for catalytic alkene hydrogenations, though hydride complexes were not isolated.[75] Peters has proposed a transient four-coordinate iron hydride complex that adds across an aromatic C=C bond of benzene,[76] and Ohki and Tatsumi have proposed the intermediacy of Cp*FeH in the cleavage of N=N bonds.[77] These precedents imply that the high activity of the isolable low-coordinate iron-hydride complexes described here is likely to have broader generality to other supporting ligands.

Reductive Elimination of Dihydrogen. Numerous polyhydride complexes, both monometallic and multimetallic, are capable of formal reduction through loss of H_2 when a ligand is added.[78] Some synthetic hydride complexes have been observed to lose H_2 with the addition of N_2.[79,80] Specifically with iron, a few polyhydride complexes reductively eliminate H_2 with ligand binding.[25,81] Iron-dihydrogen complexes have been studied in octahedral systems.[82] The reactions typically involve reduction of iron(II) to iron(0), not to iron(I) as observed here. In a recent paper, Peters has presented evidence supporting reversible metalation of a ligand alkyl group in a low-coordinate iron(I) complex.[23b]

We see no evidence of stable H_2 complexes in thermal or photochemical elimination reactions of the diketiminate-supported iron hydride complexes, because any putative transient "LFe" or "$LFe(H_2)$" is trapped by N_2 (in the photochemical reaction) or the added ligand (thermal reactions with CO or CNR). The thermal reactions must proceed through a mechanism in which substrate binding *precedes* H_2 loss, because **1a** and **1b** are stable at room temperature in solution and under vacuum. We infer that interaction with ligands activates the iron hydride species toward H_2 loss. As described above in the context of alkene/alkyne insertion, the available evidence suggests that $[L^{Me}FeH]_2$ reacts through a low-population isomer in which one iron−hydrogen bond has opened in the Fe_2H_2 core. The subsequent $L^{Me}Fe(substrate)(\mu\text{-}H)Fe(H)L^{Me}$ complex could be unstable with respect to breaking the remaining Fe−H bond to give an iron(I) product and an unstable iron(III) dihydride complex $L^{Me}FeH_2$, which could lose H_2 leading to the remaining iron(I) product. Though other mechanisms are consistent with the data, this is a working model for further studies of these reactions; it also rationalizes why the stronger ligands and those more resistant to insertion reactions (isocyanides, benzo[*c*]cinnoline, some azides) lead to iron(I) products. In the case of Me_3SiN_3, the product is not the iron(I) compound itself, but instead the result of reductive coupling of trimethylsilyl groups in Me_3SiN_3. Because the reductive coupling product also results from treatment of Me_3SiN_3 with the iron(I) source LFeNNFeL, iron(I) species are likely intermediates in this reaction.

The product of the reaction of **1a** with benzo[*c*]cinnoline is especially interesting. Despite the presence of lone pairs on the two nitrogen atoms of this heterocycle, the iron coordinates instead to the π-system. There are only four previous crystal structures in which benzo[*c*]cinnoline is a ligand to a transition metal: Ti and Yb complexes with the metal in the plane of the aromatic rings,[83] a complex with the diazene bridging the iron atoms in a $Fe_2(CO)_6$ fragment,[84] and the cobalt(0) complex $(PMe_3)_3Co(benzo[c]cinnoline)$.[85] The latter complex is the most similar to the one shown here, from its formal d^7 electronic configuration to the similar angle between the MN_2 and aromatic planes (68° vs. 55° here).[85] We have previously shown that benzene coordinates in a η^6 binding mode in $L^{Me}Fe(C_6H_6)$,[47] but the η^2 binding of benzo[*c*]cinnoline is clearly stronger, since the benzo[c]cinnoline complex is stable in benzene solution. Why, then, is the binding stronger for the more hindered benzo[*c*]-cinnoline? Previous studies on the binding constants of alkenes, alkynes, and other ligands to the iron(I) $L^{Me}Fe$ fragment showed that backbonding dominates the selectivity of binding.[57] Because of the greater electronegativity of nitrogen than carbon, the stabilizing shift of electron density from the iron to the unsaturated ligand is more effective in the iron(I) complex of benzo[c]cinnoline.

We also note that strongly hydridic M−H bonds like those in **1a** and **1b** are characteristic of early transition metal hy-

(73) (a) Field, L. D.; George, A. V.; Pike, S. R. *Polyhedron* **1995**, *14*, 3133–3137.
(74) Hillhouse, G. L.; Bercaw, J. E. *Organometallics* **1982**, *1*, 1025–1029.
(75) (a) Bart, S. C.; Lobkovsky, E.; Chirik, P. J. *J. Am. Chem. Soc.* **2004**, *126*, 13794–13807. (b) Bart, S. C.; Hawrelak, E. J.; Lobkovsky, E.; Chirik, P. J. *Organometallics* **2005**, *24*, 5518–5527. (c) Archer, A. M.; Bouwkamp, M. W.; Cortez, M.-P.; Lobkovsky, E.; Chirik, P. J. *Organometallics* **2006**, *25*, 4269–4278.
(76) Brown, S. D.; Peters, J. C. *J. Am. Chem. Soc.* **2004**, *126*, 4538–4539.
(77) Ohki, Y.; Takikawa, Y.; Hatanaka, T.; Tatsumi, K. *Organometallics* **2006**, *25*, 3111–3113.
(78) For an iron-containing example, see: Gao, Y.; Holah, D. G.; Hughes, A. N.; Spivak, G. J.; Havighurst, M. D.; Magnuson, V. R.; Polyakov, V. *Polyhedron* **1997**, *16*, 2797−2807.
(79) (a) MacKay, B. A.; Munha, R. F.; Fryzuk, M. D. *J. Am. Chem. Soc.* **2006**, *128*, 9472–9483. (b) Fryzuk, M. D.; MacKay, B. A.; Patrick, B. O. *J. Am. Chem. Soc.* **2003**, *125*, 3234–3235. (c) Fryzuk, M. D.; Johnson, S. A.; Patrick, B. O.; Albinati, A.; Mason, S. A.; Koetzle, T. F. *J. Am. Chem. Soc.* **2001**, *123*, 3969–3937.
(80) Fryzuk, M. D.; Love, J. B.; Rettig, S. J.; Young, V. G. *Science* **1997**, *275*, 1445–1447.
(81) Gilbertson, J. D.; Szymczak, N. K.; Crossland, J. L.; Miller, W. K.; Lyon, D. K.; Foxman, B. M.; Davis, J.; Tyler, D. R. *Inorg. Chem.* **2007**, *46*, 1205–1214.
(82) (a) Hills, A.; Hughes, D. L.; Jimenez-Tenorio, M.; Leigh, G. J. *J. Organomet. Chem.* **1990**, *391*, C41–C44. (b) Evans, D. J.; Jimenez-Tenorio, M.; Leigh, G. J. *J. Chem. Soc., Dalton Trans.* **1991**, 1785–1787. (c) Hills, A.; Hughes, D. L.; Jimenez-Tenorio, M.; Leigh, G. J.; McGeary, C. A.; Rowley, A. T.; Bravo, M.; McKenna, C. E.; McKenna, M.-C. *J. Chem. Soc., Chem. Commun.* **1991**, 522–524. (d) Hills, A.; Hughes, D. L.; Jimenez-Tenorio, M.; Leigh, G. J.; Rowley, A. T. *J. Chem. Soc., Dalton Trans.* **1993**, 3041–3049. (e) Helleren, C. A.; Henderson, R. A.; Leigh, G. J. *J. Chem. Soc., Dalton Trans.* **1999**, 1213–1220. (f) Hughes, D. L.; Leigh, G. J.; McMahon, C. N. *J. Chem. Soc., Dalton Trans.* **1999**, 909–914.
(83) (a) Nakayama, Y.; Nakamura, A.; Mashima, K. *Chem. Lett.* **1997**, *26*, 803–804. (b) Hill, J. E.; Fanwick, P. E.; Rothwell, I. P. *Inorg. Chem.* **1991**, *30*, 1143–1144.
(84) Doedens, R. J. *Inorg. Chem.* **1970**, *9*, 429–436.
(85) Klein, H. F.; Helwig, M.; Karnop, M.; Koenig, H.; Hammerschmitt, B.; Cordier, G.; Floerke, U.; Haupt, H. J. *Z. Naturforsch. B* **1993**, *48*, 785–793.

drides,[86] consistent with the $Fe^{\delta+}-X^{\delta-}$ character of iron alkyl, amido, and alkoxo complexes demonstrated in our earlier studies,[30,52,57] Further research will show whether the reactivity of other low-coordinate late-metal systems will also tend to mimic the behavior of transition metals with a lower *d* electron count.

Protonation To Give Dihydrogen. Many iron−hydride complexes are protonated by acids to release H_2. For example, in iron complexes of a PNP ligand, the necessary pK_a of the acid was determined to be less than 10.5 (a coordinated nitrogen was protonated in preference to the hydride ligand).[87,88] On the other hand, the diketiminate-bound iron hydrides are protonated by weak acids such as diisopropylaniline and diphenylhydrazine.[27] Using literature values in DMSO,[64] one can conclude that acids with pK_a value up to 32 (and perhaps higher) can protonate **1a** and **1b**.

Protonation of a hydride ligand may be a key step in nitrogen fixation by nitrogenases. In this hypothesis, one of the metal-bound hydride ligands is protonated and released as dihydrogen to open a coordination site for dinitrogen binding.[89] This hypothesis is consistent with Hoffman's ENDOR-based conclusion that the N_2 binding form of the iron−molybdenum cofactor is at the E_4H_2 state.[6] There are a number of acidic Arg residues near the binding face of the iron−molybdenum cofactor.[3] This hypothesis finds support here, in that weak acids are capable of protonating the hydride ligand to form H_2.

Insight into Potential Nitrogenase Mechanisms. Some nitrogenase researchers have explained the production of H_2 by nitrogenase during N_2 reduction as the result of ligand-assisted reductive elimination.[3] In this model, creation of hydrides provides a way for the FeMoco to store electrons for N_2 reduction without reaching an unrealistically low charge and reduction potential. Release of H_2 from the FeMoco is thought to be concurrent with N_2 binding, explaining why H_2 is a competitive inhibitor of N_2 reduction.[7] Other substrates are not inhibited by H_2 because the extra "boost" in reducing power from H_2 loss is not necessary. The reactivity of complexes **1a** and **1b** can be viewed using this model, in that they have sufficient reducing power to react thermally with all nitrogenase substrates except N_2. Thus, the reactivity of compounds **1** mimics not the E_4 state, but a less reduced FeMoco intermediate (E_2 or E_3) that reduces alternative substrates like alkynes, CO_2, cyanide, and azide. Photolysis of the hydride complexes **1a** and **1b** provides the "boost" required to bind the weak ligand N_2.

Even though **1a** and **1b** do not reduce N_2, their reducing power is superior to octahedral Fe−H complexes, a difference that might arise from the low coordination number, the high-spin electronic configuration, the weak Fe−H bond strength, or (most likely) a combination of these effects. Considering that iron atoms in the FeMoco have a low-coordinate geometry and high-spin electronic configuration, these factors are clearly identified as reasonable targets for evaluation in the enzyme.

It is notable that nitrogenase inhibitors (or analogues thereof) like CO, RNC, and RN_3 typically cause the synthetic hydride complexes **1a** and **1b** to *lose* H_2 and bind the small molecule that was added. Therefore, one may hypothesize that these small molecules might inhibit enzymatic N_2 reduction by binding strongly to the FeMoco, causing premature loss of H_2. The addition of **1a** and **1b** to small molecules that are substrates of nitrogenase (or analogues thereof), like RCN, alkynes, RN_3, and RN═NR, typically *forms a new substrate-H bond*, and no H_2 is lost. An exception is benzo[*c*]cinnoline: although it mimics the nitrogenase substrate diazene, it displaces H_2 like an inhibitor. This may be attributed to the aromatic nature of benzo[*c*]cinnoline,[90] which perhaps makes it more resistant to reduction than other diazenes. Azides and cyanides are inhibitors *and* substrates in the enzyme, and in the synthetic compounds they sometimes give H_2 and sometimes are reduced. Therefore, the reactions of the synthetic compounds **1a** and **1b** recall the bifurcated reactivities of these molecules with the enzyme.

It is also worth comparing the specific products of substrate reduction by nitrogenase and the products from the synthetic iron complexes. The synthetic compounds typically do not complete the reduction and release the appropriate product, but maintain a bond between the iron atom and the partially reduced substrate. For example, **1a** and **1b** reduce alkynes to iron−vinyl complexes, but do not release alkene. They reduce one C═O bond of CO_2, but do not eliminate water to give CO.[91] They reduce C≡N bonds to C═N bonds, but do not continue the reduction to methylamine or methane/ammonia. These outcomes may be attributable to the absence of protons in the synthetic system that would release the anionic ligand, either as a product or as an intermediate that is subsequently reduced to the final product. Future studies will examine the further transformations of these small molecules at iron.

Conclusions

In summary, we have shown that the first isolable low-coordinate iron hydride complexes are highly reactive toward various unsaturated small molecules. The reactions can be categorized into three types: (1) insertions of a multiple bond of the substrate into the Fe−H bond with two-electron reduction of the substrate; (2) reductive elimination of H_2 and coordination (or one-electron reduction) of the substrate; (3) loss of H^- to an acidic proton of the substrate, releasing H_2 and giving an iron complex of the conjugate base. Some of the products isolated have novel structural features, such as a square-planar iron(I) complex, a face-bound complex of benzo[*c*]cinnoline, and a monoalkylated triazenido complex. The reaction patterns are reminiscent of elementary steps in the proposed nitrogenase catalytic mechanism and support the idea that hydrides on the low-coordinate, high-spin iron atoms of the FeMoco would be capable of some of the characteristic reactions of the FeMoco. In addition, these studies identify some possible reasons why certain small molecules are substrates of nitrogenases and others are inhibitors.

Experimental Section

General Procedures. All manipulations were performed under a nitrogen atmosphere by Schlenk techniques or in an M. Braun

(86) Hoskin, A. J.; Stephan, D. W. *Coord. Chem. Rev.* **2002**, *233−234*, 107–129.
(87) (a) Henry, R. M.; Shoemaker, R. K.; Newell, R. H.; Jacobsen, G. M.; DuBois, D. L.; Rakowski-DuBois, M. *Organometallics* **2005**, *24*, 2481–2491. (b) Jacobsen, G. M.; Shoemaker, R. K.; Rakowski-DuBois, M.; DuBois, D. L. *Organometallics* **2007**, *26*, 4964–4971.
(88) (a) Dihydrogen complexes are often strong acids, for example: Jia, G.; Morris, R. H. *J. Am. Chem. Soc.* **1991**, *113*, 875–883. (b) Cappellani, E. P.; Drouin, S. D.; Jia, G.; Maltby, P. A.; Morris, R. H.; Schweitzer, C. T. *J. Am. Chem. Soc.* **1994**, *116*, 3375–3388.
(89) (a) Henderson, R. A. *Chem. Commun.* **1987**, 1670–1672. (b) Hlatky, G. G.; Crabtree, R. H. *Coord. Chem. Rev.* **1985**, *65*, 1–48. (c) Oglieve, K. E.; Henderson, R. A. *Chem. Commun.* **1992**, 441–443.
(90) Husseini, A.; Akasheh, T. S. *Dirasat. Univ. Jordan* **1985**, *12*, 65–72.
(91) We are not aware that any researchers have investigated the reduction of formate by nitrogenase. This would be a fruitful area of investigation.

glovebox maintained at or below 1 ppm of O_2 and H_2O. Glassware was dried at 150 °C overnight. NMR data were recorded on a Bruker Avance 500 spectrometer (500 MHz). All peaks in the NMR spectra are referenced to residual protiated solvents (benzene δ 7.16 ppm; toluene δ 2.08 ppm; cyclohexane δ 1.38 ppm). In parentheses are listed integrations and assignments. Resonances were singlets unless otherwise specified. Infrared spectra (450−4000 cm^{-1}) were recorded on KBr pellet samples in a Shimadzu FTIR spectrophotometer (FTIR-8400S) using 32 scans at 2 cm^{-1} resolution. UV−vis spectra were measured on a Cary 50 spectrophotometer using screw-cap cuvettes; descriptions of the spectra include extinction coefficients in parentheses. Solution magnetic susceptibilities were determined by the Evans method.[92] Elemental analyses were determined by Desert Analytics, Tucson, AZ.

Pentane, tetrahydrofuran (THF), diethyl ether, and toluene were purified by passage through activated alumina and "deoxygenizer" columns from Glass Contour Co. (Laguna Beach, CA). Deuterated solvents were first dried over CaH_2, then over Na/benzophenone, and then vacuum transferred into a storage container. Before use, an aliquot of each solvent was tested with a drop of sodium benzophenone ketyl in THF solution. Celite was dried overnight at 200 °C under vacuum. CO_2 was purchased from Air Products, dried by passing through 4Å molecular sieves, and freed from O_2 with three freeze−pump−thaw cycles. H_2O, ^{t}BuNC, ^{t}BuCN, MeCN, and 2,6-diisopropylphenylamine were degassed before using. Diphenylacetylene, benno[*c*]cinnoline, and 1-azidoadamantane (AdN_3) were crystallized from pentane in the glovebox. Compounds **1a** and **1b** were prepared by published procedures.[20,21]

$L^{Me}Fe(CN^tBu)_2$ (2a). Reaction of **1a** and ^{t}BuNC in C_6D_6 gives complex **2a**, in a crude yield of 62% based on ^{1}H NMR integration with an internal integration standard. However, it can be more conveniently synthesized from $L^{Me}FeNNFeL^{Me}$ and ^{t}BuNC as follows. A solution of $L^{Me}FeNNFeL^{Me}$ (205 mg, 0.21 mmol) in pentane (15 mL) was treated with ^{t}BuNC (105 μL, 0.93 mmol) with stirring. Immediate bubbling was observed and the solution color changed from deep brown to bright orange. The reaction solution was stirred at ambient temperature for 5 h. Volatile materials were removed under vacuum and the residue was extracted with pentane (20 mL) and filtered through Celite. The solution was concentrated to 3 mL and cooled to −35 °C to give bright orange crystals of **2a** (145 mg, 54%). ^{1}H NMR (500 MHz, C_6D_6): δ 9.1 (2H, aryl *p*-H), 5.8 (4H), 3.5 (12H, ^{i}Pr-CH_3), 2.5 (18H, ^{t}Bu), 1.3 (4H), −2.0 (6H, backbone CH_3), −5.8 (12H, ^{i}Pr-CH_3) ppm. (Peaks integrated as 4H could be aryl *m*-H or ^{i}Pr methine CH; the backbone CH was not observed). UV−vis (pentane): 317 (25.3 mM^{-1} cm^{-1}), 447 (3.9 mM^{-1} cm^{-1}), 808 (0.2 $mM^{-1}cm^{-1}$) nm. IR (KBr pellet): 2122 (vs), 2050 (m), 1969 (m), 1948 (m) cm^{-1}. The X-band EPR spectrum is shown in the Supporting Information. Attempts to measure the solution magnetic moment of **2a** were not successful because the internal standard peak was obscured. Complex **2a** is thermally unstable (decomposition of a solid sample occurred overnight inside the glovebox), and all characterizations were done with fresh samples. The instability prevented elemental analysis measurements.

$L^{Me}Fe(\mu\text{-}N{=}CHMe)_2FeL^{Me}$ (3a). A stirring solution of $[L^{Me}FeH]_2$ (**1a**) (146 mg, 0.15 mmol) in toluene (30 mL) was treated with MeCN (18.0 μL, 0.34 mmol). The reaction solution was heated at 45 °C for 18 h and the color changed from deep brown to yellow. All volatile materials were removed under vacuum and the residue was extracted with toluene (30 mL), filtered, and concentrated to 5 mL. Cooling to −35 °C gave orange-yellow crystals of **3a** (155 mg, 88%). ^{1}H NMR (500 MHz, C_7D_8): δ 50 (6H, N=CHCH_3), 20 (12H), 13 (4H), 12 (4H), −2 (12H), −7 (12H), −12 (4H), −16 (4H), −21 (12H), −22 (4H), −31 (2H, diketiminate backbone), −40 (12H) ppm. (No peak corresponding to the imine proton was identified. Peaks integrated as 4H could be ^{i}Pr methine, aryl *p*-H, or aryl *o*-H; peaks integrated as 12H could be ^{i}Pr-CH_3 or backbone CH_3). UV−vis (toluene): 337 (34.2 mM^{-1} cm^{-1}), 392 (4.8 mM^{-1} cm^{-1}) nm. IR (KBr pellet): 1637 cm^{-1} (C=N). μ_{eff} (1% $Me_3SiOSiMe_3$ in THF-d_8, 25 °C): 5.9(1) μ_B per dimer. Anal. Calcd for $C_{62}H_{90}N_6Fe_2$: C, 72.22; H, 8.80; N, 8.15. Found: C, 72.04; H, 8.98; N, 7.72.

$L^{Me}Fe(\eta^1\text{-}N{=}CH^tBu)(\mu\text{-}H)FeL^{Me}$ (4a). A solution of **1a** (100 mg, 0.11 mmol) in pentane (10 mL) was treated with ^{t}BuCN (12.0 μL, 0.11 mmol) and stirred at room temperature for 2 h. Volatile materials were removed under vacuum and the residue was extracted with toluene (30 mL), filtered, and concentrated to 5 mL. Crystallization at −35 °C gave **4a** as a brown powder (97 mg, 85%). ^{1}H NMR (500 MHz, C_6D_6): The narrow range of the NMR spectrum, the broad peaks, and the low symmetry of the molecule led to severe overlap between peaks, which made assignment unsuccessful. The spectrum is shown in the Supporting Information. UV−vis (pentane): 332 (30 mM^{-1} cm^{-1}). IR (KBr pellet): 1629 cm^{-1} (C=N). Anal. Calcd for $C_{63}H_{93}N_5Fe_2$: C, 73.31; H, 9.08; N, 6.79. Found: C, 73.50; H, 9.40; N, 6.46.

$L^{tBu}Fe(N{=}CH^tBu)$ (5b). A solution of **1b** (91 mg, 81 μmol) in diethyl ether (8 mL) was treated with ^{t}BuCN (18 μL, 163 μmol) and stirred at room temperature for 30 min. The volatile materials were removed under vacuum. The orange residue was extracted with toluene, filtered through Celite, concentrated, and stored at −35 °C to afford **5b** as orange-red crystals (70 mg, 67%). ^{1}H NMR (500 MHz, C_6D_6): δ 95 (9H, ^{t}Bu of imide), 92 (1H, backbone C−H), 36 (18H, ^{t}Bu of diketiminate), 3 (4H, m-Ar), −24 (12H, ^{i}Pr-CH_3), −99 (4H, ^{i}Pr-CH), −103 (12H, ^{i}Pr-CH_3), −108 (2H, p-Ar) ppm. There was no clear peak for NC*H*^{t}Bu. UV−vis (toluene): 335 (25 mM^{-1} cm^{-1}), 397 (6.7 mM^{-1} cm^{-1}), 454 (sh), 515 (sh) nm. μ_{eff} (C_6D_6, 298 K): 4.6 μ_B. IR (KBr pellet): 3058 (w), 2960 (vs), 2906 (w), 2867 (m), 2717 (w), 2631 (w), 1687 (s), 1506 (s), 1462 (w), 1433 (w), 1383 (vs), 1362 (vs), 1317 (s), 1255 (w), 1217 (w), 1182 (w), 1151 (w), 1095 (m), 1024 (w) cm^{-1}. Anal. Calcd for $C_{40}H_{63}FeN_3$: C, 74.86; H, 9.89; N, 6.55. Found: C, 74.52; H, 9.80; N, 6.80.

L^{Me}Fe-hexyl. In a J. Young NMR tube, **1a** (5.6 mg, 5.9 μmol) and 1-hexene (1.5 μL, 12.1 μmol) were dissolved in 0.5 mL of C_6D_6. After 1 h, a single paramagnetic species was observed by ^{1}H NMR spectroscopy: δ 116 (2H), 77 (1H, backbone CH), 51 (2H), 33 (6H, diketiminate CH_3), 32 (3H, hexyl CH_3), 15 (4H), −19 (12H, ^{i}Pr-CH_3), −21 (4H), −30 (2H), −44 (2H), −75 (12H, ^{i}Pr-CH_3), −91 (2H) ppm. Peaks integrated as 4H could be aryl *m*-H or ^{i}Pr methine CH; peaks integrated as 2H could be aryl *p*-H, hexyl β-CH_2, γ-CH_2, δ-CH_2, or ϵ-CH_2. The hexyl α-CH_2 protons were not observed in the ^{1}H NMR spectrum. This ^{1}H NMR spectrum is very similar to the spectra of other L^{Me}Fe(alkyl) species we have previously reported.[30]

$L^{Me}Fe(CPh{=}CHPh)$ (6a). A mixture of **1a** (88 mg, 93 μmol) and PhCCPh (33 mg, 187 μmol) in pentane (15 mL) was stirred at room temperature for 17 h. Volatile materials were removed under vacuum. The product was extracted with pentane (20 mL), filtered through Celite, and concentrated to 2 mL. Cooling to −35 °C gave **6a** as a yellow powder (87 mg, 75%). ^{1}H NMR (500 MHz, C_6D_6): δ 123 (1H), 60 (1H), 59 (2H), 57 (6H, diketiminate CH_3), 51 (1H), 48 (2H), 33 (2H), −9 (4H), −19 (12H, ^{i}Pr CH_3), −78 (2H), −118 (12H + 4H, ^{i}Pr CH_3 + another peak, possible assignments are listed below) ppm. Peaks integrated as 4H could be aryl *m*-H or ^{i}Pr methine CH; peaks integrated as 2H could be aryl *p*-H, vinyl phenyl *m*-H (2 peaks for the two phenyl groups), or phenyl *o*-H; peaks integrated as 1H could be backbone CH, vinyl phenyl *p*-H (2 peaks for the two phenyl groups). The vinyl C=CH and *o*-H from the vinyl phenyl closer to the iron were not observed. μ_{eff} (C_6D_6, 298 K) = 5.15(2) μ_B. UV−vis (pentane): 320 (37.9 mM^{-1} cm^{-1}), 495 (1.5 mM^{-1} cm^{-1}) nm.

$L^{tBu}Fe(\mu\text{-}N_3)_2FeL^{tBu}$ (7b). A solution of **1b** (71 mg, 64 μmol) in diethyl ether (10 mL) was treated with Me_3SiN_3 (18 μL, 128 μmol) and stirred at room temperature for 2 h. An orange precipitate formed within 30 min. The volatile materials were removed under vacuum. The orange residue was extracted with hot toluene and filtered through Celite while hot to give an orange solution. This solution was concentrated and cooled to −35 °C to afford **7b** as

orange crystals (70 mg, 79%). **7b** is insoluble in benzene, and slightly soluble in toluene, at room temperature. ^{1}H NMR (500 MHz, C_7D_8, 75 °C): δ 15, 1, −3, −24, −46 ppm. The broadness of the peaks prevented accurate integration and assignment of the peaks. μ_{eff} (C_7D_8, 348 K): 4.1 μ_B. IR (KBr pellet): 2962 (s), 2929 (w), 2869 (m), 2129 (vs), 2081 (w), 1529 (w), 1490 (m), 1463 (w), 1436 (w), 1380 (m), 1357 (s), 1317 (s), 1259 (m), 1215(w), 1190 (w), 1097 (m), 1054 (w), 1024 (m) cm^{-1}. UV−vis (toluene): 337 (15.5 mM^{-1}cm^{-1}) nm. Anal. Calcd for $C_{70}H_{106}N_{10}Fe_2$: C, 70.10; H, 8.91; N, 11.68. Found: C, 70.04; H, 8.71; N, 11.02.

L$^{t\mathrm{Bu}}$Fe(HNNNAd) (8b). A solution of **1b** (88 mg, 79 μmol) in diethyl ether (8 mL) was treated with a solution of AdN_3 (28 mg, 157 μmol) in diethyl ether (5 mL) and stirred at room temperature for 30 min to give an orange-red solution. The volatile materials were removed under vacuum. The residue was extracted with toluene and filtered through Celite. This solution was concentrated and cooled to −35 °C to afford L$^{t\mathrm{Bu}}$Fe(HNNNAd) as brown crystals (77 mg, 67%). ^{1}H NMR (500 MHz, C_6D_6): δ 39 (3H, Ad-α, β, or γ), 21 (18H, ^{t}Bu), 15 (4H, *m*-Ar), 10 (3H, Ad- α, β, or γ), 8 (3H, Ad-α, β, or γ), 3.7 (3H, Ad-α, β, or γ), −7 (12H, ^{i}Pr-CH$_3$), −27 (1H, NH), −40 (12H, ^{i}Pr-CH$_3$), −51 (3H, Ad-α, β, or γ), −61 (2H, p-H) ppm. UV−vis (toluene): 340 (18 mM^{-1} cm^{-1}), 415 (sh), 530 (sh) nm. μ_{eff} (C_6D_6, 298 K) 4.6 μ_B. IR (KBr pellet): 3371 (w), 3059 (w), 2960 (vs), 2926 (s), 2905 (vs), 2850 (m), 1622 (w), 1585 (w), 1526 (w), 1491 (s), 1464 (m), 1429 (w), 1380 (vs), 1356 (vs), 1311 (m), 1263 (w), 1215 (w), 1182 (w), 1153 (w), 1099 (m), 1022 (m) cm^{-1}. Elemental analysis could not be obtained for this compound as **8b** is thermally unstable.

Thermal Conversion of 8b to L$^{t\mathrm{Bu}}$FeNHAd. A sample of **8b** (∼5 mg) in C_6D_6 was heated to 80 °C for 5 h. The ^{1}H NMR spectrum was identical to a sample prepared independently through the following method. A mixture of L$^{t\mathrm{Bu}}$FeCl (257 mg, 0.433 mmol), LiNHAd (68 mg, 0.43 mmol), and diethyl ether (10 mL) was stirred at room temperature for 2 h. The yellow-orange solution was filtered through Celite, and the volatile materials were removed under vacuum. The orange residue was dissolved in *n*-hexane (3 mL), and cooling the solution to −45 °C afforded L$^{t\mathrm{Bu}}$FeNHAd as bright orange crystals in 2 crops (230 mg, 75%). ^{1}H NMR (500 MHz, C_6D_6): δ 95 (6H, Ad-α), 67 (3H, Ad-β or γ), 42 (3H, Ad-β or γ), 37 (18H, ^{t}Bu), 31 (3H, Ad-β or γ), −1 (4H, *m*-Ar), −24 (12H, ^{i}Pr-C*H*$_3$), −93 (4H, ^{i}Pr-C*H*), −102 (2H, *p*-Ar), −118 (12H, ^{i}Pr-CH$_3$) ppm. The N-*H* and backbone C-*H* protons were not located. μ_{eff} (C_6D_6, 298 K): 4.6(3) μ_B. IR (KBr pellet): 3277 (w, ν_{N-H}), 3052 (w), 3013 (w), 2959 (vs), 2925 (s), 2903 (vs), 2845 (m), 1534 (m), 1502 (s), 1459 (m), 1443 (m), 1430 (m), 1385 (vs), 1364 (vs), 1319 (s), 1303 (m), 1253 (w), 1218 (m), 1197 (m), 1131 (m), 1095 (s), 1055 (m), 1029 (m), 948 (w), 933 (w), 890 (w) cm^{-1}. UV−vis (pentane): 340 (14 mM^{-1} cm^{-1}), 510 (sh, ∼0.4 mM^{-1} cm^{-1}) nm.

L$^{\mathrm{Me}}$Fe(benzo[*c*]cinnoline) (9a). Although reaction of **1a** and benzo[*c*]cinnoline gives complex **9a** (yield 90% by ^{1}H NMR spectroscopy), it is more easily synthesized from L$^{\mathrm{Me}}$FeNNFeL$^{\mathrm{Me}}$ and benzo[*c*]cinnoline. A vial was loaded with L$^{\mathrm{Me}}$FeNNFeL$^{\mathrm{Me}}$ (94 mg, 96 μmol) and benzo[*c*]cinnoline (35 mg, 190 μmol). Pentane (15 mL) was added, causing an immediate color change from brown to green. The reaction solution was stirred at room temperature for 5 h, filtered through Celite, concentrated to 3 mL, and cooled to −35 °C to give dark green plates of **9a** (113 mg, 91%). ^{1}H NMR (500 MHz, C_6D_{12}): δ 140 (4H), 111 (4H), 17 (12H, ^{i}Pr-CH$_3$), −17 (6H, backbone CH$_3$), −21 (4H), −52 (12H, ^{i}Pr-CH$_3$), −78 (2H, *p*-Ar) ppm (peaks integrated as 4H could be *m*-Ar, ^{i}Pr CH, or overlapped peaks for benzo[*c*]cinnoline ligand). UV−vis: 305 (16.3 mM^{-1} cm^{-1}), 325 (13.1 mM^{-1} cm^{-1}), 388 (9.7 mM^{-1} cm^{-1}), 419 (7.0 mM^{-1} cm^{-1}), 585 (2.3 mM^{-1} cm^{-1}) nm. μ_{eff} (C_6D_6, 25 °C): 3.1(1) μ_B. Anal. Calcd for $C_{41}H_{49}N_4Fe$: C, 75.33; H, 7.55; N, 8.57. Found: C, 73.31; H, 7.68; N, 7.98. Repeated attempts at elemental analysis did not give better agreement, indicating a possible small impurity not visible by NMR spectroscopy.

L$^{\mathrm{Me}}$Fe(μ-OCHO)$_2$FeL$^{\mathrm{Me}}$ (10a). A resealable flask was loaded with **1a** (254 mg, 0.27 mmol) and pentane (15 mL). CO_2 (256 mbar, 61.7 mL, 0.64 mmol) was condensed in the reaction flask at 77 K over 30 min. The flask was warmed to room temperature and stirred for 22 h. Volatile materials were removed from the yellow mixture under vacuum and the residue was extracted with toluene (30 mL), filtered, and concentrated to 5 mL. Cooling to −35 °C gave yellow blocks of **10a** (138 mg, 50%). ^{1}H NMR (500 MHz, C_6D_6): δ 18 (4H), 5 (12H, ^{i}Pr CH$_3$), −11 (12H + 4H, ^{i}Pr CH$_3$ + another 4H; possible assignments for this 4H peak are listed below), −19 (1H, backbone CH), −42 (2H, aryl *p*-H), −60 (6H, backbone CH$_3$) ppm. (Peaks integrated as 4H could be aryl *m*-H or ^{i}Pr methine CH; the two bridging formate H were not observed in the NMR spectrum). UV−vis (pentane): 332 (ϵ = 29.9 mM^{-1} cm^{-1}) nm. IR: 1628 cm^{-1} (C−O). μ_{eff} (C_6D_6, 25 °C): 8.8(1) μ_B per dimer. Anal. Calcd for $C_{60}H_{84}N_4O_4Fe_2$: C, 69.49; H, 8.16; N, 5.40. Found: C, 73.52; H, 9.52; N, 5.62. Repeated attempts at elemental analysis did not give better agreement, indicating a possible small impurity not visible by NMR spectroscopy.

L$^{t\mathrm{Bu}}$Fe(μ-OCHO)$_2$FeL$^{t\mathrm{Bu}}$ (10b). This was identical to the synthesis of **10a**, but using **1b** (17 mg, 15 μmol), diethyl ether (15 mL), and CO_2 (99 mbar; 7.73 mL, 30 μmol). The yield of **10b** was 15 mg (82%). ^{1}H NMR (500 MHz, C_7D_8, 85 °C) δ 30 (1, backbone C−H), 19 (18H, ^{t}Bu), 16 (4H, ^{i}Pr-CH), −8 (12H, ^{i}Pr-CH$_3$), −42 (12H, ^{i}Pr-CH$_3$), −50 (2H, *p*-H or O$_2$CH), −70 (2H, *p*-H or O$_2$CH) ppm. A 4H peak for the *m*-Ar protons was not observed, and is possibly obscured by the solvent. UV−vis (toluene): 339 (43 mM^{-1} cm^{-1}), 393 (6.0 mM^{-1} cm^{-1}), 516 (sh) nm. IR (KBr pellet): 3059 (w), 2962 (vs), 2929 (s), 2869 (m), 1626 (vs), 1529 (w), 1493 (s), 1462 (m), 1437 (m), 1381 (vs), 1360 (vs), 1317 (s), 1259 (m), 1215 (w), 1190 (w), 1157 (w), 1099 (s), 1024 (s) cm^{-1}. Anal. Calcd. for $C_{72}H_{108}Fe_2N_4O_4$: C, 71.75; H, 9.03; N, 4.65. Found: 72.79; H, 8.63; N, 4.68.

L$^{t\mathrm{Bu}}$Fe(^{i}PrNCHN^{i}Pr) (11b). A solution of **1b** (57 mg, 51 μmol) in diethyl ether (8 mL) was treated with *N*,*N*′-diisopropylcarbodiimide (15.8 μL, 102 μmol) and stirred for 1 h. The reaction mixture turned orange within a couple of minutes. The volatile materials were removed under vacuum. The resultant orange solid was extracted with toluene, filtered through Celite, concentrated, and stored at −35 °C to afford orange-red crystals of **11b** (62 mg, 89%). ^{1}H NMR (500 MHz, C_6D_6): δ 142 (2H, *p*-Ar), 120 (1H, backbone C−H of diketiminate), 19 (4H, *m*-Ar or ^{i}Pr-CH), 10 (18H, ^{t}Bu), 5 (12H, ^{i}Pr-CH$_3$), 2.9 (12H, ^{i}Pr-CH$_3$), 2.0 (4H, *m*-H or ^{i}Pr-CH), −9 (12H, ^{i}Pr-CH$_3$), −36 (2H, ^{i}Pr-CH of amidinate), −85 (1H, backbone C−H of amidinate) ppm. UV−vis (toluene): 349 (14 mM^{-1} cm^{-1}), 405 (10.2 mM^{-1} cm^{-1}), 475 (sh) nm. μ_{eff} (C_6D_6, 298 K) 4.2(3) μ_B. IR (KBr pellet): 3057 (w), 2962 (vs), 2929 (w), 2867 (m), 1657 (w), 1547 (s), 1479 (m), 1460 (m), 1431 (w), 1382 (vs), 1360 (s), 1317 (m), 1257 (vs), 1191 (w), 1097 (m), 1020 (s) cm^{-1}. Anal. Calcd for $C_{42}H_{68}FeN_4$: C, 73.66; H, 10.01; N, 8.18. Found: C, 73.80; H, 10.42; N, 8.10.

[L$^{\mathrm{Me}}$Fe(μ-OH)]$_2$ (12a). To a solution of **1a** (189 mg, 0.20 mmol) in THF (10 mL), a solution of H_2O in THF (0.28 mM, 1.45 mL, 0.41 mmol) was added dropwise with stirring. Bubbling was observed and the solution turned to green. The solution was stirred at room temperature for 20 h. Volatile materials were removed under vacuum with heating at 120 °C. The residue was extracted with pentane (20 mL), filtered, and concentrated to 5 mL. Cooling to −35 °C gave a green powder, which was further dried under vacuum with heating at 120 °C for 10 h to give dry **12a** (131 mg, 67%). ^{1}H NMR (500 MHz, C_6D_6): δ 9 (4H), 4 (12 H, ^{i}Pr-CH$_3$), −5 (1H, backbone CH), −6 (6H, diketiminate CH$_3$), −8 (4H), −33 (2H, aryl *p*-H), −38 (12H, ^{i}Pr-CH$_3$) ppm (peaks integrated as 4H could be ^{i}Pr-CH or aryl *o*-H; the bridging OH protons are not observed.). UV−vis (pentane): 326 (27.1 mM^{-1} cm^{-1}) nm. IR (KBr pellet): 3709, 3668 cm^{-1} (O−H). μ_{eff} (C_6D_6, 25 °C): 7.5(1) μ_B per dimer. Anal. Calcd for $C_{58}H_{84}N_4O_2Fe_2$: C, 71.01; H, 8.63; N, 5.71. Found: C, 71.11; H, 8.72; N, 5.53.

Detection of H_2 Using Gas Chromatography.[28] The reaction solution from a given reaction in 3 mL of toluene was performed in a 25 mL round-bottom flask. The flask was capped by an adapter with a stopcock leading to a rubber septum. Using a syringe, 8 mL of the gas inside was removed and 8 mL of CH_4 (1043 mbar) was injected into the flask as an internal standard. An aliquot (20 μL) of the gas was withdrawn and injected into a GC (Shimadzu GC-17A) with a 5 Å molecular sieve column (30 m × 0.25 mm) at 26 °C, carrier gas N_2, 600 kPa. The ratio of integrated H_2/CH_4 responses were compared to a calibration plot previously determined[28] by injecting known amounts of H_2 into the same flask with 3 mL of toluene.

Mössbauer Spectroscopy. Mössbauer data were recorded on a spectrometer with alternating constant acceleration. The minimum experimental line width was 0.24 mm/s (full width at half-height). The sample temperature was maintained constant either in an Oxford Instruments Variox or an Oxford Instruments Mössbauer-Spectromag cryostat. The latter is a split-pair superconducting magnet system for applied fields up to 8 T where the temperature of the sample can be varied in the range 1.5−250 K. The field at the sample is perpendicular to the γ-beam. The ^{57}Co/Rh source (1.8 GBq) was positioned at room temperature inside the gap of the magnet system at a zero-field position. Isomer shifts are quoted relative to iron metal at 298 K. Magnetic Mössbauer spectra for the paramagnetic contamination of **1a** were simulated by using a spin-Hamiltonian description of the electronic ground state:

$$H_e = D[S_{t,z}^2 - S_t(S_t + 1)/3 + (E/D)(S_{t,x}^2 - S_{t,y}^2)] + \mu_B \mathbf{B} \cdot S_t \quad (1)$$

where S_t is the total spin of the system, and D and E/D are the axial and rhombic zero-field parameters. The hyperfine interactions for ^{57}Fe were calculated by using the usual nuclear Hamiltonian.[93] For **1a** only the nuclear Hamiltonian was used.

Computational Methods. The Gaussian 03 package[94] was used for all calculations described herein. Hybrid quantum mechanics/molecular mechanics (QM/MM) calculations were used to study full experimental models of $L^{Me}Fe(CN^tBu)_2$. The QM/MM calculations utilized the ONIOM[95] methodology. The MM region was modeled with the universal force field (UFF)[96] and included the Ar and Me substituents of $L^{Me,Ar}$ and the methyl groups of ^{t}BuNC. The remainder of $L^{Me}Fe(CN^tBu)_2$ was modeled at the B3LYP/6-311+G(d) level of theory. Geometries were fully optimized using gradient methods unless otherwise noted. The unrestricted Kohn−Sham formalism was used for the description of all open-shell species. The energy Hessian was calculated for all stationary points and thus confirmed the calculated stationary points as minima (no imaginary frequencies). All reported enthalpies are calculated at 1 atm and 298.15 K.

Acknowledgment. This work was supported by grants from the National Institutes of Health (Grant GM065313 to P.L.H.) and the National Science Foundation (Grant CHE-0701247 to T.R.C.), as well as a Sloan Research Fellowship (P.L.H.) and a Weissberger Fellowship (Y.Y.). We thank Bernd Mienert for collection of Mössbauer data. Calculations employed the UNT computational chemistry resource, whose purchase was supported by a NSF CRIF grant (CHE-0342824).

Supporting Information Available: Complete ref 94; spectra (PDF) and crystallographic data (CIF). This material is available free of charge via the Internet at http://pubs.acs.org.

JA710669W

(92) (a) Schubert, E. M. *J. Chem. Educ.* **1992**, *69*, 62. (b) Evans, D. F. *J. Chem. Soc.* **1959**, 2003–2005.
(93) Trautwein, A. X.; Bill, E.; Bominaar, E. L.; Winkler, H. *Struct. Bonding (Berlin)* **1991**, *78*, 1–95.
(94) Frisch, M. J. et al. *Gaussian 03*; Gaussian Inc.: Pittsburgh, PA, 1998.
(95) Svensson, M.; Humbel, S.; Froese, R. D. J.; Matsubara, T.; Sieber, S.; Morokuma, K. *J. Phys. Chem.* **1996**, *100*, 19357–19363.
(96) (a) Rappé, A. K.; Casewit, C. J.; Colwell, K. S.; Goddard, W. A.; Skiff, W. M. *J. Am. Chem. Soc.* **1992**, *114*, 10024–10035. (b) Casewit, C. J.; Colwell, K. S.; Rappé, A. K. *J. Am. Chem. Soc.* **1992**, *114*, 10035–10046.